

## 2. AUSTRALIAN $\delta^{13}\text{C}_{\text{org}}$ -ISOTOPE PROFILES ABOUT THE PERMIAN-TRIASSIC BOUNDARY

Stratigraphically well placed samples from coreholes have been used to develop  $\delta^{13}\text{C}_{\text{org}}$  depth profiles through the Permian from palynological Stage 3b Zone (Artinskian) to the palynological *Samaropollenites speciosus* Zone (Norian) in the Triassic. Samples are from conventional core unless otherwise indicated. Core material was used because the most complete Permian-Triassic marine sections in Australia are thought to be those from the northwest offshore Bonaparte Basin and are hence unavailable from outcrop and because core samples are less likely to have suffered the effects of weathering which may be present in outcrop samples. The cored sections also contain suitable fossils for biostratigraphic correlation against one another. The section locations are listed in Table 2.0 and the location of the sedimentary basins studied are shown on Fig. 2.0 The sample interval depth, depositional environment, and palynological control on sections is summarised in Table 2.1. Fig. 2.1 shows the equivalence of palynological zones. The Permian-Triassic boundary placements as suggested by various authors relative to the palynological zones is indicated.

Two additional sections from Gondwanaland, one from New Zealand and the other from South Africa, are reviewed in Appendix 2.1.

The analytical procedures used to determine  $\delta^{13}\text{C}_{\text{org}}$  and TOC are described in Appendix 2.2. All  $\delta^{13}\text{C}_{\text{org}}$ ,  $\delta^{13}\text{C}_{\text{CO}_3}$  and  $\delta^{18}\text{O}_{\text{CO}_3}$  values are in permil (‰) relative to the PDB standard.

**Table 2.0** Basins, sub-basins, wells, and latitudes and longitudes.

Basin	Sub Basin	Well name	Latitude S	Longitude E
Bonaparte	Petrel	Tern 3	13° 20' 10"	128° 06' 16"
Bonaparte	Petrel	Fishburn 1	12° 58' 04.711"	127° 35' 03.624"
Bonaparte	Petrel	Petrel 4	12° 53' 18.21"	128° 29' 41.16"
Bonaparte	Ashmore Block	Sahul Shoals 1	11° 25' 36"	124° 32' 50"
Canning	Fitzroy Trough	Paradise Cores	18° 01' approx.	124° 31' approx.
Carnarvon	Ashburton	Onslow 1	21° 45' 56"	114° 52' 17"
Perth	Northern	BMR 10 (Beagle Ridge)	29° 49' 38"	114° 58' 30"
Perth	Bunbury Trough	Whicher Range 2	33° 50' 19"	115° 22' 18"
Cooper		Merrimelia 3	27° 37' 25"	140° 21' 28"
Bowen	Denison Trough	Denison NS 20	23° 32' 11"	148° 09' 34"
Bowen	Denison Trough	GSQ Eddystone 1	25° 20' approx.	148° 18' approx.
Bowen	Denison Trough	GSQ Eddystone 5	25° 00' approx.	148° 29' approx.
Bowen	Denison Trough	GSQ Taroom 10	25° 13' approx.	148° 47' approx.
Bowen	Denison Trough	GSQ Springsure 19	24° 41' 16"	148° 08' 26"
Sydney	Macdonald Syncline	DM Murrays Run DDH1	33° 06' approx.	151° 11' approx.
Sydney		Lisarow DDH 1	33° 22' 38.5"	151° 23' 0.5"
Sydney		DM Awaba DDH 2	33° 01' 34.8"	151° 34' 27.8"
Sydney		Bunnerong DDH1	33° 58' 18.5"	151° 13' 44"
Sydney		DM Newvale DDH 28	33° 12' 50" approx.	151° 34' approx.

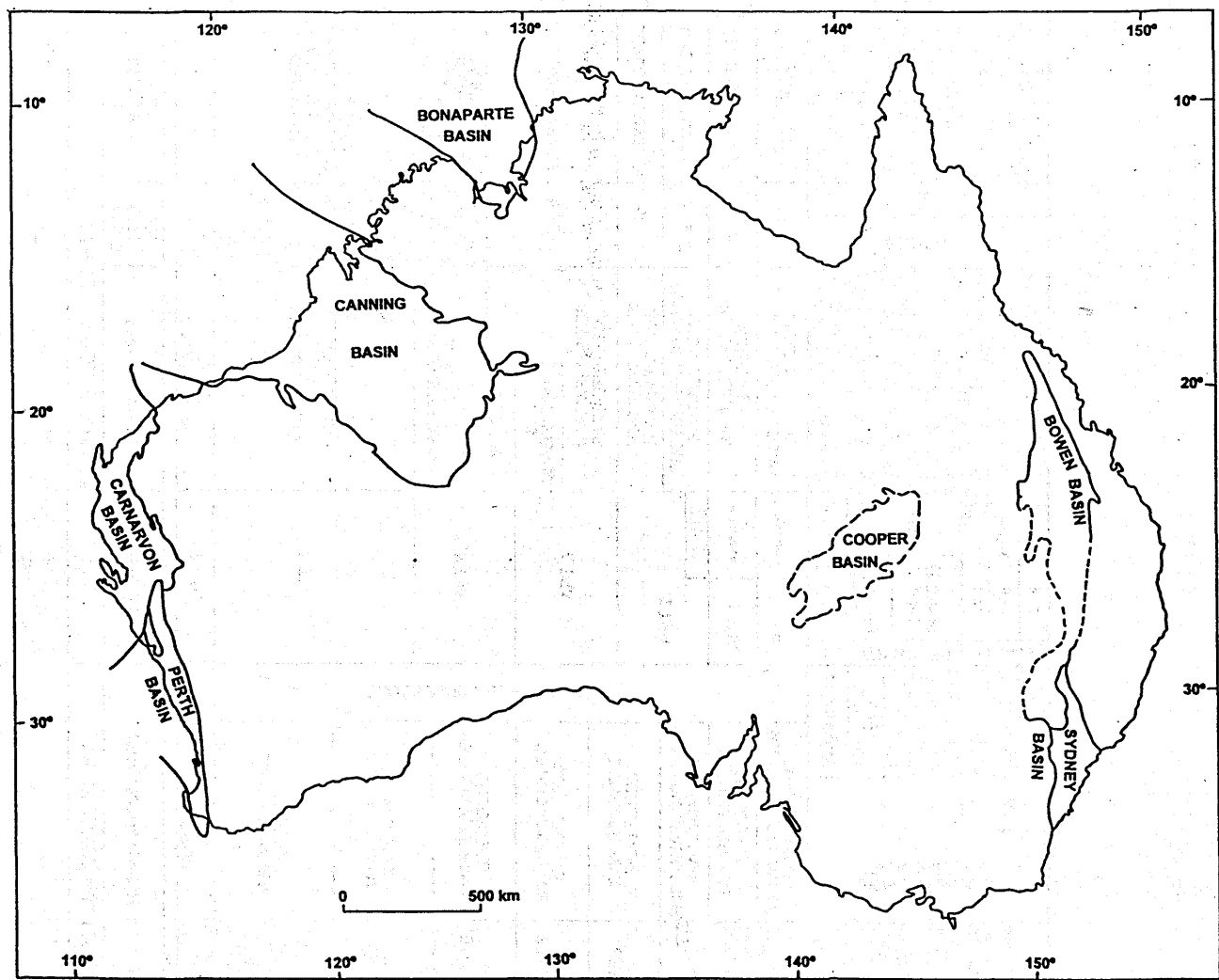


Figure 2.0 Location of Australian sedimentary basins sampled.

Figure 2.1 Distribution of sedimentary basins in Australia. The map shows the location of the basins and the distribution of the sedimentary basins in Australia. The basins are labeled as Bonaparte Basin, Canning Basin, Carnarvon Basin, Perth Basin, Cooper Basin, Bowen Basin, and Sydney Basin. The map also shows the distribution of the sedimentary basins in Australia.

Fig.2.1

DINOFLAGELLATE ZONES WEST			SPORE-POLLEN ZONES WEST			SPORE-POLLEN ZONES EAST			AGE						
Helby et al., 1987		Balme 1984	Dolby & Balme, 1976		Helby et al., 1987, 1975	Price et al., 1985 Price, 1983	Helby et al., 1987	Evans 1986, 1987	Helby 1970, 1973 1975						
SHUBLIKODINIUM SUPERZONE			PTERUCHIPOLLENITES			FALCISPORITES SUPERZONE			LATE						
											COROLLINA TOROSA		APT 1	COROLLINA TOROSA	UNNAMED BLUNDAMBA COAL MEASURES ASSEMBLAGE
											ASHMORIPOLLIS REDUCTA		APT 5	POLYINGULATISPORITES CRENULATUS	
											MINUTOSACCUS CRENULATUS				APT 4
											SAMAROPOLLENITES SPECIOSUS		APT 3	QUADRIFIDUS	
											STAUIROSACCITES QUADRIFIDUS				APT 2
											TIGRISPORITES PLAYFORDII		APT 1	LUNATISPORITES PELLUCIDUS	
											KRAEUSELISPORITES SAEPTATUS				PP 6
											TAENIAE-SPORITES		PP 5-4 U5 b-c (=PP5.2) U5 a (=PP5.1) L5c L5b L5a	P3c PP 5 L5c L5b L5a	
											DULHUNTYISPORIA				Weylandites Kemp et al., 1977
DULHUNTYISPORIA			DULHUNTYISPORIA ASSEMBLAGE			B		A							
DULHUNTYISPORIA			DULHUNTYISPORIA ASSEMBLAGE			Weylandites Kemp et al., 1977		P3c PP 5 L5c L5b L5a		STAGES 5 P4					
DULHUNTYISPORIA			DULHUNTYISPORIA ASSEMBLAGE			Weylandites Kemp et al., 1977		P3c PP 5 L5c L5b L5a		STAGES 5 P4					
DULHUNTYISPORIA			DULHUNTYISPORIA ASSEMBLAGE			Weylandites Kemp et al., 1977		P3c PP 5 L5c L5b L5a		STAGES 5 P4					
DULHUNTYISPORIA			DULHUNTYISPORIA ASSEMBLAGE			Weylandites Kemp et al., 1977		P3c PP 5 L5c L5b L5a		STAGES 5 P4					
DULHUNTYISPORIA			DULHUNTYISPORIA ASSEMBLAGE			Weylandites Kemp et al., 1977		P3c PP 5 L5c L5b L5a		STAGES 5 P4					
DULHUNTYISPORIA			DULHUNTYISPORIA ASSEMBLAGE			Weylandites Kemp et al., 1977		P3c PP 5 L5c L5b L5a		STAGES 5 P4					
DULHUNTYISPORIA			DULHUNTYISPORIA ASSEMBLAGE			Weylandites Kemp et al., 1977		P3c PP 5 L5c L5b L5a		STAGES 5 P4					
DULHUNTYISPORIA			DULHUNTYISPORIA ASSEMBLAGE			Weylandites Kemp et al., 1977		P3c PP 5 L5c L5b L5a		STAGES 5 P4					
DULHUNTYISPORIA			DULHUNTYISPORIA ASSEMBLAGE			Weylandites Kemp et al., 1977		P3c PP 5 L5c L5b L5a		STAGES 5 P4					
DULHUNTYISPORIA			DULHUNTYISPORIA ASSEMBLAGE			Weylandites Kemp et al., 1977		P3c PP 5 L5c L5b L5a		STAGES 5 P4					
DULHUNTYISPORIA			DULHUNTYISPORIA ASSEMBLAGE			Weylandites Kemp et al., 1977		P3c PP 5 L5c L5b L5a		STAGES 5 P4					
DULHUNTYISPORIA			DULHUNTYISPORIA ASSEMBLAGE			Weylandites Kemp et al., 1977		P3c PP 5 L5c L5b L5a		STAGES 5 P4					
DULHUNTYISPORIA			DULHUNTYISPORIA ASSEMBLAGE			Weylandites Kemp et al., 1977		P3c PP 5 L5c L5b L5a		STAGES 5 P4					
DULHUNTYISPORIA			DULHUNTYISPORIA ASSEMBLAGE			Weylandites Kemp et al., 1977		P3c PP 5 L5c L5b L5a		STAGES 5 P4					
DULHUNTYISPORIA			DULHUNTYISPORIA ASSEMBLAGE			Weylandites Kemp et al., 1977		P3c PP 5 L5c L5b L5a		STAGES 5 P4					
DULHUNTYISPORIA			DULHUNTYISPORIA ASSEMBLAGE			Weylandites Kemp et al., 1977		P3c PP 5 L5c L5b L5a		STAGES 5 P4					
DULHUNTYISPORIA			DULHUNTYISPORIA ASSEMBLAGE			Weylandites Kemp et al., 1977		P3c PP 5 L5c L5b L5a		STAGES 5 P4					
DULHUNTYISPORIA			DULHUNTYISPORIA ASSEMBLAGE			Weylandites Kemp et al., 1977		P3c PP 5 L5c L5b L5a		STAGES 5 P4					
DULHUNTYISPORIA			DULHUNTYISPORIA ASSEMBLAGE			Weylandites Kemp et al., 1977		P3c PP 5 L5c L5b L5a		STAGES 5 P4					
DULHUNTYISPORIA			DULHUNTYISPORIA ASSEMBLAGE			Weylandites Kemp et al., 1977		P3c PP 5 L5c L5b L5a		STAGES 5 P4					
DULHUNTYISPORIA			DULHUNTYISPORIA ASSEMBLAGE			Weylandites Kemp et al., 1977		P3c PP 5 L5c L5b L5a		STAGES 5 P4					
DULHUNTYISPORIA			DULHUNTYISPORIA ASSEMBLAGE			Weylandites Kemp et al., 1977		P3c PP 5 L5c L5b L5a		STAGES 5 P4					
DULHUNTYISPORIA			DULHUNTYISPORIA ASSEMBLAGE			Weylandites Kemp et al., 1977		P3c PP 5 L5c L5b L5a		STAGES 5 P4					
DULHUNTYISPORIA			DULHUNTYISPORIA ASSEMBLAGE			Weylandites Kemp et al., 1977		P3c PP 5 L5c L5b L5a		STAGES 5 P4					
DULHUNTYISPORIA			DULHUNTYISPORIA ASSEMBLAGE			Weylandites Kemp et al., 1977		P3c PP 5 L5c L5b L5a		STAGES 5 P4					
DULHUNTYISPORIA			DULHUNTYISPORIA ASSEMBLAGE			Weylandites Kemp et al., 1977		P3c PP 5 L5c L5b L5a		STAGES 5 P4					
DULHUNTYISPORIA			DULHUNTYISPORIA ASSEMBLAGE			Weylandites Kemp et al., 1977		P3c PP 5 L5c L5b L5a		STAGES 5 P4					
DULHUNTYISPORIA			DULHUNTYISPORIA ASSEMBLAGE			Weylandites Kemp et al., 1977		P3c PP 5 L5c L5b L5a		STAGES 5 P4					
DULHUNTYISPORIA			DULHUNTYISPORIA ASSEMBLAGE			Weylandites Kemp et al., 1977		P3c PP 5 L5c L5b L5a		STAGES 5 P4					
DULHUNTYISPORIA			DULHUNTYISPORIA ASSEMBLAGE			Weylandites Kemp et al., 1977		P3c PP 5 L5c L5b L5a		STAGES 5 P4					
DULHUNTYISPORIA			DULHUNTYISPORIA ASSEMBLAGE			Weylandites Kemp et al., 1977		P3c PP 5 L5c L5b L5a		STAGES 5 P4					
DULHUNTYISPORIA			DULHUNTYISPORIA ASSEMBLAGE			Weylandites Kemp et al., 1977		P3c PP 5 L5c L5b L5a		STAGES 5 P4					
DULHUNTYISPORIA			DULHUNTYISPORIA ASSEMBLAGE			Weylandites Kemp et al., 1977		P3c PP 5 L5c L5b L5a		STAGES 5 P4					
DULHUNTYISPORIA			DULHUNTYISPORIA ASSEMBLAGE			Weylandites Kemp et al., 1977		P3c PP 5 L5c L5b L5a		STAGES 5 P4					
DULHUNTYISPORIA			DULHUNTYISPORIA ASSEMBLAGE			Weylandites Kemp et al., 1977		P3c PP 5 L5c L5b L5a		STAGES 5 P4					
DULHUNTYISPORIA			DULHUNTYISPORIA ASSEMBLAGE			Weylandites Kemp et al., 1977		P3c PP 5 L5c L5b L5a		STAGES 5 P4					
DULHUNTYISPORIA			DULHUNTYISPORIA ASSEMBLAGE			Weylandites Kemp et al., 1977		P3c PP 5 L5c L5b L5a		STAGES 5 P4					
DULHUNTYISPORIA			DULHUNTYISPORIA ASSEMBLAGE			Weylandites Kemp et al., 1977		P3c PP 5 L5c L5b L5a		STAGES 5 P4					
DULHUNTYISPORIA			DULHUNTYISPORIA ASSEMBLAGE			Weylandites Kemp et al., 1977		P3c PP 5 L5c L5b L5a		STAGES 5 P4					
DULHUNTYISPORIA			DULHUNTYISPORIA ASSEMBLAGE			Weylandites Kemp et al., 1977		P3c PP 5 L5c L5b L5a		STAGES 5 P4					
DULHUNTYISPORIA			DULHUNTYISPORIA ASSEMBLAGE			Weylandites Kemp et al., 1977		P3c PP 5 L5c L5b L5a		STAGES 5 P4					
DULHUNTYISPORIA			DULHUNTYISPORIA ASSEMBLAGE			Weylandites Kemp et al., 1977		P3c PP 5 L5c L5b L5a		STAGES 5 P4					
DULHUNTYISPORIA			DULHUNTYISPORIA ASSEMBLAGE			Weylandites Kemp et al., 1977		P3c PP 5 L5c L5b L5a		STAGES 5 P4					
DULHUNTYISPORIA			DULHUNTYISPORIA ASSEMBLAGE			Weylandites Kemp et al., 1977		P3c PP 5 L5c L5b L5a		STAGES 5 P4					
DULHUNTYISPORIA			DULHUNTYISPORIA ASSEMBLAGE			Weylandites Kemp et al., 1977		P3c PP 5 L5c L5b L5a		STAGES 5 P4					
DULHUNTYISPORIA			DULHUNTYISPORIA ASSEMBLAGE			Weylandites Kemp et al., 1977		P3c PP 5 L5c L5b L5a		STAGES 5 P4					
DULHUNTYISPORIA			DULHUNTYISPORIA ASSEMBLAGE			Weylandites Kemp et al., 1977		P3c PP 5 L5c L5b L5a		STAGES 5 P4					
DULHUNTYISPORIA			DULHUNTYISPORIA ASSEMBLAGE			Weylandites Kemp et al., 1977		P3c PP 5 L5c L5b L5a		STAGES 5 P4					
DULHUNTYISPORIA			DULHUNTYISPORIA ASSEMBLAGE			Weylandites Kemp et al., 1977		P3c PP 5 L5c L5b L5a		STAGES 5 P4					
DULHUNTYISPORIA			DULHUNTYISPORIA ASSEMBLAGE			Weylandites Kemp et al., 1977		P3c PP 5 L5c L5b L5a		STAGES 5 P4					

Figure 2.1 Equivalence of palynological zonation schemes referred to in this study. Different placements of the Permian-Triassic boundary are indicated A; at the base of the *P. microcorpus* Zone (traditional following David and Browne, 1950), B at the top of the *P. microcorpus* Zone following Helby et al. (1987), and C at the base of the *Protohaploxypinus samoilovichii* Zone associated with the appearance of *Aratrisporites* (Foster, 1982).

**Table 2.1.** Summary of the sections studied with interpreted environment of deposition at the Permian-Triassic boundary, depth range from which samples were analysed (approximately), and the quality of biostratigraphical control based on palynology.

BASIN	WELL	ENVIRONMENT OF DEPOSITION	DEPTH RANGE OF WELL SECTIONS SAMPLED m	PALYNOLOGY CONTROL
Bonaparte	Tern- 3	Marine	2350 - 2520	Good
	Fishburn-1	Marine	1830 - 2860	Good
	Petrel-4	paralic?	3300 - 3820	Good
	Sahul Shoals-1	Marine	1850-3800	Spot
Canning	Paradise Cores	Marginal marine	17 - 350	Good
Carnarvon	Onslow -1	Marine	1900 -2300	Spot
Bowen	Denison NS-20	Fluvial	360 - 480	Good
	Eddystone-1	Fluvial/marine	150 - 950	Good
	Taroom-10	Marine	830 -970	Good
	Eddystone-5	Marine	550 - 1350	Good
Perth	Whicher Range-1	Fluvial	3475 - 4000	Spot
	BMR -10	Marine	680 - 980	Good
Sydney	Murrays Run-1	Fluvial/lacustrine	50 -800	Good
	Lisarow-1	Fluvial/lacustrine	635 -670	Spot
	Bunnerong-1	Fluvial/lacustrine	730 - 900	Spot
	Newvale-28	Fluvial/lacustrine	75 -110	Spot

## 2.1 Bonaparte Basin

The Bonaparte Basin in northwest Australia, extends from onshore to offshore, covers approximately 270 000 km<sup>2</sup> and contains 18 km of Phanerozoic sedimentary and volcanic rocks (Mory, 1990). The latest Permian and Triassic development of the basin was associated with an interior sag followed by a northeast to southwest rift (Mory, 1990). This study is confined to the Permian Fossil Head and Hyland Bay Formations and the Triassic Mount Goodwin, Osprey, Pollard and Challis Formations. Sedimentation was in a deltaic, shallow to open marine or estuarine environment (Table 2.2) (Mory, 1990).

Samples from four wells drilled in the offshore Bonaparte Basin (Tern-3, Fishburn-1, Petrel-4, and Sahul Shoals-1) (Fig. 2.2) range from Permian palynological Zone Stage 3b to the Late Triassic (Norian) palynological *Samaropollenites speciosus* Zone (Nicoll and Foster, 1994, fig. 4).

Table 2.2 Bonaparte Basin stratigraphy modified from Mory (1990).

Unit	Stratigraphic relationships	Age	Depositional environment
Challis Formation	Conformable on Pollard Fm.	late Ladinian to Carnian	Open-marine shelf
Pollard Formation	Conformable on Osprey Fm.	late Anisian to early Carnian	Open-marine shelf
Osprey Formation.	Conformable on Mt Goodwin Formation	mid to late Anisian	Open marine shelf
Mount Goodwin Formation	Conformable on Hyland Bay Formation	?Scythian to ?early Anisian	Open marine
Hyland Bay Formation	Conformable to disconformable on the Fossil Head Formation	Kungurian to late Tatarian	Deltaic, barrier bar, alluvial and marine shelf.
Fossil Head Formation	Conformable on Keyling Formation	Artinskian to Kungurian.	Marine shelf

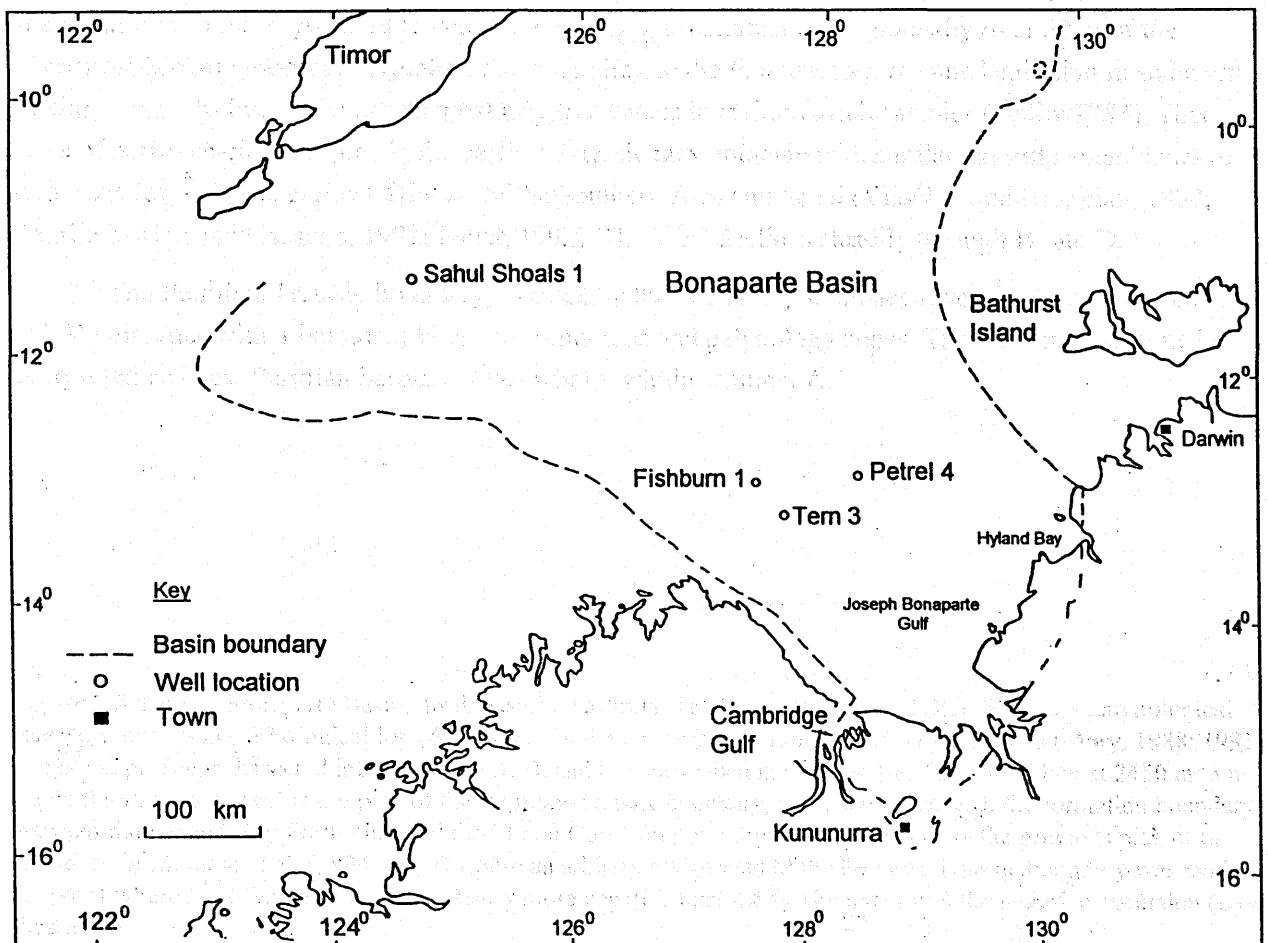


Fig. 2.2 Locations of Tern-3, Petrel-4, Fishburn-1, and Sahul Shoals-1 in the Bonaparte Basin.

### 2.1.1 Tern-3

Tern-3 (Fig. 2.3, Table 2.3) was drilled in 1982 in NT/P28 to investigate the petroleum prospectivity of a salt diapir. It penetrated the marine Early Triassic Mount Goodwin Formation and the underlying Late Permian Hyland Bay Formation. Palynological control (Helby, 1983) is excellent, with 75 m of the palynological *Weylandites* and 44 m of the palynological *P. microcorpus* Zone suggesting continuous or near-continuous sedimentation across the Permian-Triassic boundary. The Hyland Bay Formation was deposited in a shelf-deltaic environment and the overlying Mount Goodwin Formation in a shallow marine environment (Gunn and Ly, 1989).

In the  $\delta^{13}\text{C}_{\text{org}}$  profile (Fig. 2.3), six of the Hyland Bay Formation samples in the *Weylandites* Zone (Helby, 1983) have similar  $\delta^{13}\text{C}_{\text{org}}$  values at about -24‰, and a seventh sample at -22.1‰ has a more  $^{13}\text{C}$  - enriched value. In the overlying 35 m of the *P. microcorpus* Zone there is a marked  $\delta^{13}\text{C}_{\text{org}}$  decrease of about 10‰. This decrease in  $\delta^{13}\text{C}_{\text{org}}$  values is gradual and may coincide with the transition from more charcoal-rich organic matter that may indicate a component of older reworked material in the lower *P. microcorpus* Zone (Helby, 1983). Five of a set of six samples in the upper part of the *P. microcorpus* Zone and the lower part of the *Lunatisporites pellucidus* Zone have similar  $\delta^{13}\text{C}$  values averaging -32.2‰. The organic matter in these samples is predominantly from acritarchs and is suggestive of the typical acritarch dominated sediments found in the early "Triassic" Locker Shale in the Carnarvon Basin (Dolby and Balme, 1976) and Blina Shale in the Canning Basin (Helby, 1975). The sixth sample in the undetermined section between the *P. microcorpus* Zone and the *L. pellucidus* Zone has an even lower value of -34.5‰. Higher in the section,  $\delta^{13}\text{C}$  values increase to an average value of about -29‰ for a set of six samples in the *L. pellucidus* Zone. The  $\delta^{13}\text{C}_{\text{org}}$  excursion occurs gradually over 50 m of the lowermost Mount Goodwin Formation corresponding to the *P. microcorpus* Zone beginning in sediments lacking acritarchs but achieving its most negative values in acritarch-rich samples (Helby 1983). This spike of acritarch-rich samples in the earliest Triassic may coincide with similar extreme abundances of acritarchs found in the earliest Triassic of the Southern Alps and Israel (Visscher and Brugman, 1988; Broglio Loriga and Cassinis, 1992; Eshet, 1992). The TOC declines steadily through B into D.

The Permian-Triassic boundary, marked by the beginning of the negative  $\delta^{13}\text{C}$ -isotope excursion (A/ B) coincides with a boundary between formations and palynology zones. The *Weylandites* Zone is interpreted as latest Permian because it lies wholly within segment A.

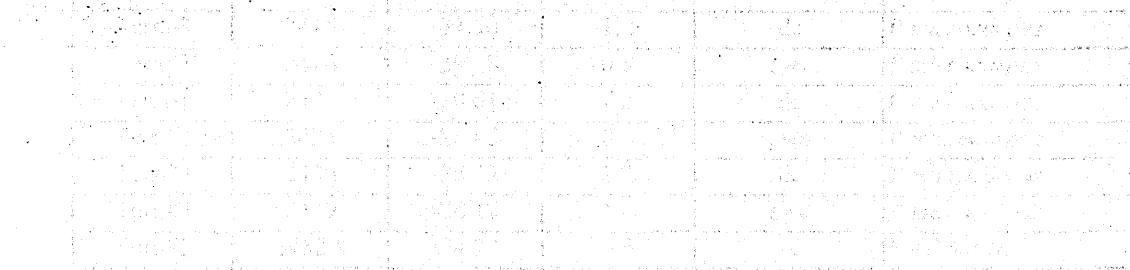
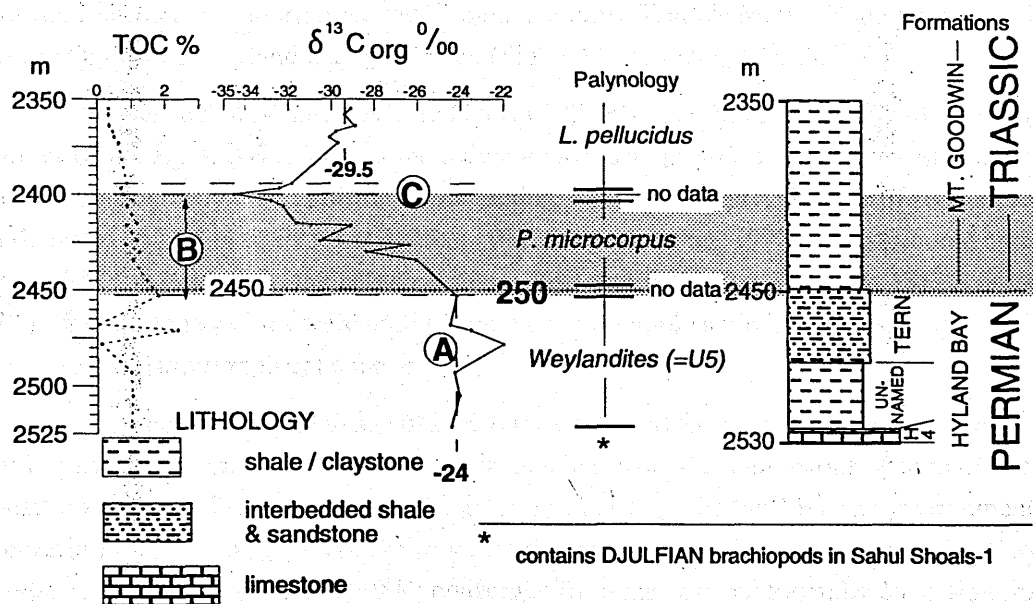


Figure 2.3 Tern-3, Bonaparte Basin, northwestern Australia. Total organic carbon (TOC),  $\delta^{13}\text{C}_{\text{org}}$ , palynological zones (Helby, 1983), lithological log (Australian Aquitaine Petroleum Ltd, 1982) and formations (Mory, 1988; 1991). The  $\delta^{13}\text{C}$  profile is dissected into segments A, B, and C as described in Chapter 1.8. The dotted line at 2450 m, 3 m above the B/A boundary, is my pick of the Permian-Triassic boundary, and it coincides with the formation boundary between the Hyland Bay Formation and the Mount Goodwin Formation. This differs from the previous pick of the boundary in Morante et al. (1994, fig. 2) where an arbitrary assignment of the Permian-Triassic boundary was made at the point where  $\delta^{13}\text{C}$  values were consistently more negative than -26‰. The interval of the negative excursion (B) is shaded.

## BONAPARTE BASIN : TERN - 3

FIG 2.3

Table 2.3 Tern 3.  $\delta^{13}C_{org}$ , TOC %, and biostratigraphy.

Well	depth m	$\delta^{13}C_{org} \text{ ‰}$	TOC%	sample type	Palynology Zone
Tern#3	2355	-29.15	0.3	dc	undetermined
Tern#3	2358	-29.43	0.3	dc	undetermined
Tern#3	2364	-28.99	0.3	dc	<i>L. pellucidus</i>
Tern#3	2367	-29.80	0.4	dc	<i>L. pellucidus</i>
Tern#3	2370	-30.14	0.5	dc	<i>L. pellucidus</i>
Tern#3	2373	-29.72	0.6	dc	<i>L. pellucidus</i>
Tern#3	2394	-31.69	0.9	dc	<i>L. pellucidus</i>
Tern#3	2397	-32.43	1.2	swc	<i>L. pellucidus</i>
Tern#3	2400	-34.54	0.8	dc	undetermined
Tern#3	2403	-32.83	1.0	swc	<i>P. microcorpus</i>
Tern#3	2406	-32.23	0.9	dc	<i>P. microcorpus</i>
Tern#3	2415	-31.70	1.2	dc	<i>P. microcorpus</i>
Tern#3	2416	-29.18	0.8	swc	<i>P. microcorpus</i>
Tern#3	2424	-30.61	1.2	dc	<i>P. microcorpus</i>
Tern#3	2426	-26.42	0.8	swc	<i>P. microcorpus</i>
Tern#3	2430	-28.42	1.2	dc	<i>P. microcorpus</i>
Tern#3	2439	-26.10	1.0	swc	<i>P. microcorpus</i>
Tern#3	2452.8	-24.24	1.8	cc	<i>Weylandites</i>
Tern#3	2467.9	-24.54	< 0.1	cc	<i>Weylandites</i>
Tern#3	2470.9	-23.69	2.4	cc	<i>Weylandites</i>
Tern#3	2477.9	-22.09	0.1	cc	<i>Weylandites</i>
Tern#3	2493	-24.34	1.0	swc	<i>Weylandites</i>
Tern#3	2505	-24.13	1.0	swc	<i>Weylandites</i>
Tern#3	2521	-24.49	1.0	swc	<i>Weylandites</i>

cc = conventional core; dc = ditch cuttings; swc = side wall core

### 2.1.2 Petrel-4

Petrel-4, drilled in 1988 to investigate a drape anticline (Gunn and Ly, 1989), penetrated a marginal marine to nonmarine section through the Early Triassic Mount Goodwin Formation and the underlying Permian Hyland Bay Formation (Figs 2.4, 2.5; Table 2.4).

The well was continuously cored (cores 1-9) from depths 3571 to 3698 m through the Cape Hay Member of the Hyland Bay Formation. Palynological data provides excellent biostratigraphical control over the continuously cored portion of the section, with the interpreted range of zone PP5.4- PP6 in core 1 at a depth of 3571.4 m to PP5.4 at 3688 m (Woods pers. comm., 1992). An additional cored interval from 3803 to 3821 m belongs to the palynostratigraphical unit PP4.3.2 at 3802.2 to 3812.3 m. Samples above 3570 m from ditch cuttings were used to complete the sample suite into the Triassic-like  $\delta^{13}\text{C}_{\text{org}}$  values but have no biostratigraphical control.

A palynostratigraphical age of PP6 was determined for a sample from core 4 at 3603.4 m, but this sample is now thought to represent contamination because of an anomalous open marine environment of deposition compared to adjacent samples interpreted as deposited in a paralic environment, and the observation that the length of core from which this sample was obtained was milled undersize (Geoff Woods, SANTOS, pers. comm., 1994; confirmed from the core photography collection for Petrel-4). The sample from 3603.4 m also has an anomalous  $\delta^{13}\text{C}_{\text{org}}$  value of -29.97‰ (encircled dot in Fig. 2.4, 2.5) compared to samples from 3598.5 m and 3608.2 m with  $\delta^{13}\text{C}_{\text{org}}$  values of -22.44 and -22.69‰ respectively.

Figure 2.4 shows an interpretation of the  $\delta^{13}\text{C}_{\text{org}}$  profile in which the negative  $\delta^{13}\text{C}_{\text{org}}$  excursion starts at 3435 m (segment A/B boundary). In this interpretation the beginning of segment B is delayed because ditch cutting samples between 3435 and 3561 m are contaminated with more negative  $\delta^{13}\text{C}_{\text{org}}$  material caved from above. Three reasons for supporting this interpretation are:

- 1) The apparent placement of the Dombey Member, Hyland Bay Formation (H4 limestone) below the  $\delta^{13}\text{C}_{\text{org}}$  excursion in this section yet above the  $\delta^{13}\text{C}_{\text{org}}$  excursion in the Fishburn-1 and Tern-3 sections.
- 2) The strongly positive  $\delta^{13}\text{C}_{\text{CO}_3}$  value (5.02‰) determined on a sample of the Dombey Member from 3540 m. Strongly positive  $\delta^{13}\text{C}_{\text{CO}_3}$  values are typical of Permian carbonates (Grossman, 1994).
- 3) Lithostratigraphical correlation with the Dombey Member in Sahul Shoals-1 (Fig. 2.7) which is known to contain brachiopods of "Chhidruan" (Djulfian) age (Archbold, 1988). This interpretation brings the magnitude of the  $\delta^{13}\text{C}_{\text{org}}$  excursion in Petrel 4 to 9‰, similar to that in Tern-3 and Fishburn-1.

In an alternative interpretation (Fig. 2.5) the beginning of the negative  $\delta^{13}\text{C}_{\text{org}}$  excursion in the corehole is at 3561 m. This interpretation indicates the  $\delta^{13}\text{C}_{\text{CO}_3}$  value (5.02 ‰) determined on a sample of the Dombey Member (= H4 limestone) from a depth of 3540 m is anomalously heavy for a sample of Triassic age and implies that the Dombey member is diachronous across the basin, because it would occur in different places above and below the  $\delta^{13}\text{C}_{\text{org}}$  excursion. This interpretation of the  $\delta^{13}\text{C}_{\text{org}}$  curve is not favoured.

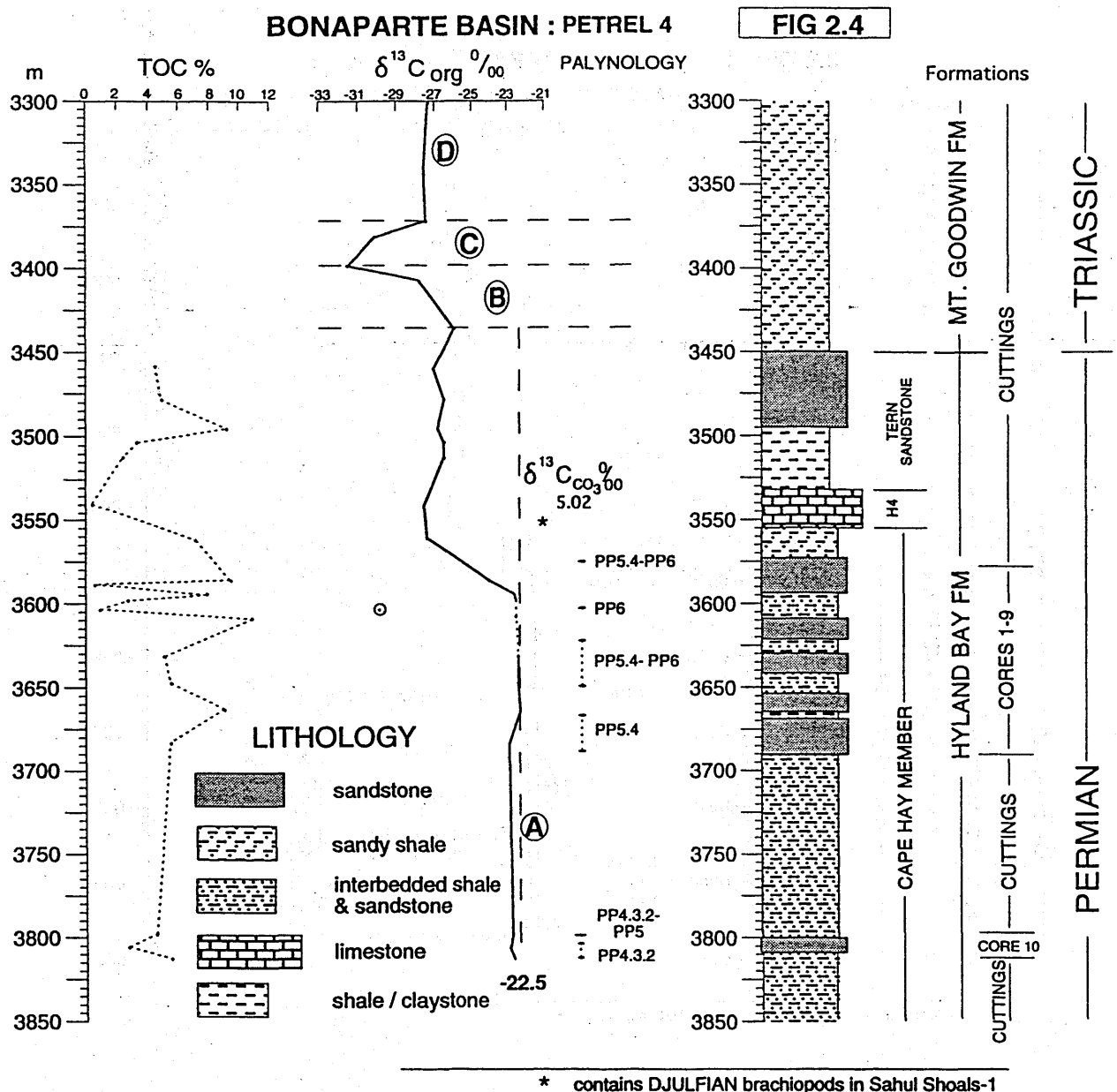
There is no clear pattern in the variation of TOC in this section below the interval of the  $\delta^{13}\text{C}$ -isotope excursion and data from the cuttings (Figs 2.4, 2.5) is unreliable as lithologies are mixed in the samples.



Table 2.4 Petrel-4.  $\delta^{13}\text{C}_{\text{org}}$ , TOC %, and biostratigraphy.

Well	depth m	$\delta^{13}\text{C}_{\text{org}}\text{‰}$	TOC%	Sample type	Palynology Zone
Petrel 4	3300	-27.13	na	dc	
Petrel 4	3344	-27.26	na	dc	
Petrel 4	3372	-27.25	na	dc	
Petrel 4	3381	-30.29	na	dc	
Petrel 4	3399	-31.46	na	dc	
Petrel 4	3408	-27.61	na	dc	
Petrel 4	3435	-25.89	na	dc	
Petrel 4	3459	-27.01	4.5	dc	
Petrel 4	3477	-26.72	5.0	dc	
Petrel 4	3495	-26.92	9.1	dc	
Petrel 4	3504	-26.53	3.5	dc	
Petrel 4	3513	-26.53	2.2	dc	
Petrel 4	3540	-27.38	>0.2	dc	
Petrel 4	3561	-27.28	7.0	dc	
Petrel 4	3585.68	-23.52	9.4	cc	PP5.4-PP6
Petrel 4	3589.08	-22.61	0.5	cc	PP5.4-PP6
Petrel 4	3593.98	-22.49	7.9	cc	PP5.4-PP6
Petrel 4	3598.5	-22.44	2.3	cc	PP5.4-PP6
Petrel 4	3603.42	-29.97	0.9	cc	PP6
Petrel 4	3608.2	-22.69	10.7	cc	PP5.4-PP6
Petrel 4	3632	-22.42	5.1	cc	PP5.4-PP6
Petrel 4	3646.6	-22.96	5.5	cc	PP5.4-PP6
Petrel 4	3664.4	-21.85	9.0	cc	PP5.4
Petrel 4	3683.6	-23.29	5.6	cc	PP5.4
Petrel 4	3798.45	-22.73	4.4	cc	PP4.3.2-PP5
Petrel 4	3806.03	-22.79	2.7	cc	PP4.3.2
Petrel 4	3813	-22.68	5.6	cc	PP4.3.2

Note. A single whole-rock limestone from 3540 m had a  $\delta^{13}\text{C}_{\text{CO}_3}$  of 5.02‰ and  $\delta^{18}\text{O}_{\text{CO}_3}$  of -6.30‰.  
cc = conventional core, dc = ditch cuttings sample.



**Figure 2.4** Petrel-4, Bonaparte Basin, northwestern Australia. Total organic carbon (TOC),  $\delta^{13}C_{org}$ , palynological zones (G. Woods, pers. comm., 1993), lithological log, and formations (SANTOS Petroleum, 1988). The negative excursion in  $\delta^{13}C_{org}$  is between mean values of -22.5 ‰ and an extreme value of -31.46 ‰ (C). The  $\delta^{13}C_{CO_3}$  value of 5.02 ‰ (asterisk) is plotted at the appropriate  $\Delta$  offset of about -27 ‰ (Magaritz et al., 1992) and supports an interpretation that the ditch cutting samples are anomalously negative because of contamination. The negative  $\delta^{13}C_{org}$  excursion between segments A and D on this curve is from averages around -22.5 to -27 ‰. The size of the extreme excursion (B) is -9 ‰.

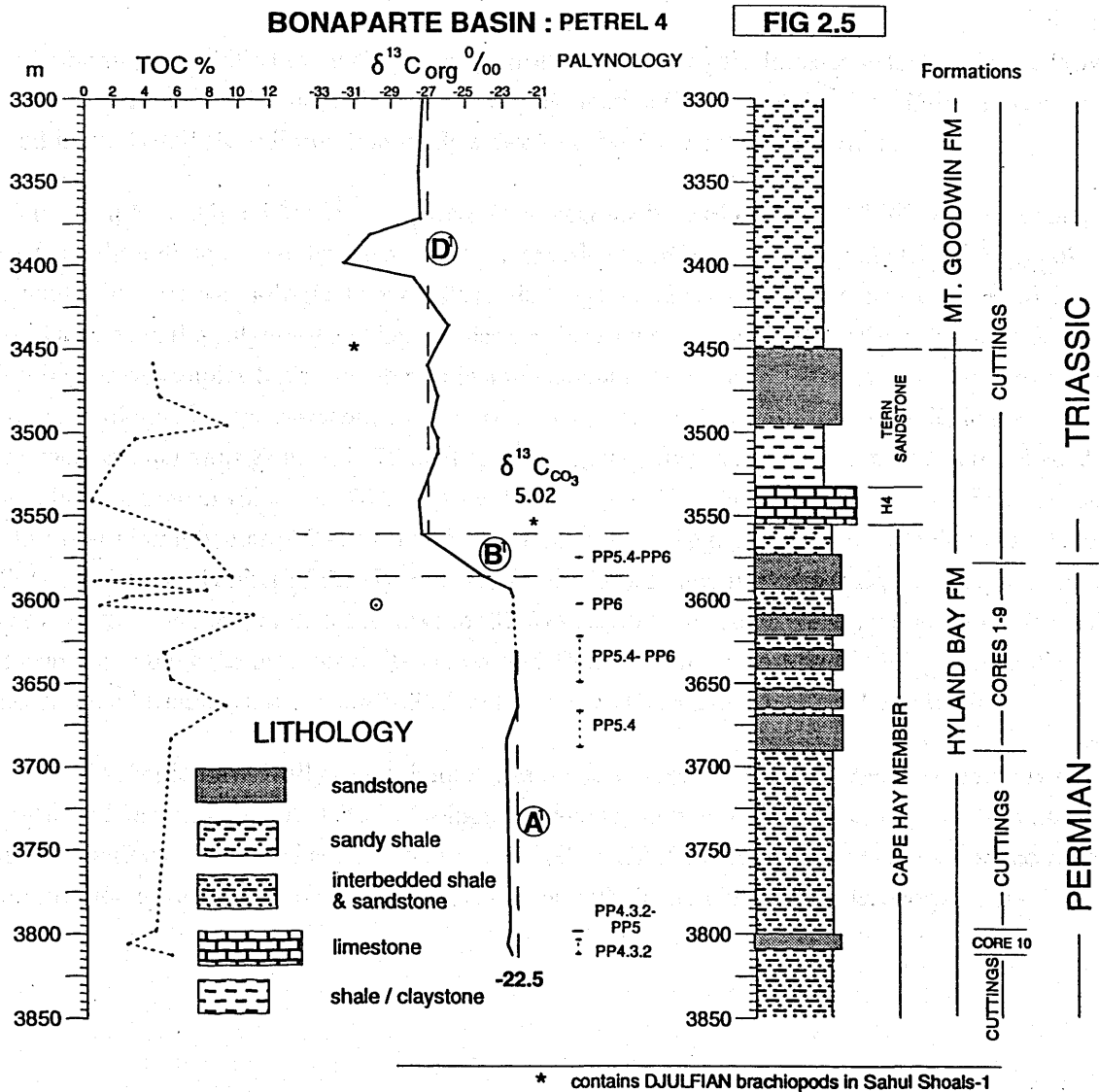


**Figure 2.5** Petrel-4, alternative interpretation. The negative excursion in  $\delta^{13}C_{org}$  is between mean values of -22.5‰ for the Permian and -27‰ for the Triassic.

### 2.1.3 Fishburn-1

Fishburn-1 was drilled in 1992 by BHP Petroleum to investigate Jurassic sandstone in the Plover Formation and Permian sandstone in the Hyland Bay Formation (Fig. 2.6, Table 2.5). Drilling was abandoned in the Fossil Head Formation. Only sidewall cores were cut during drilling.

The samples analysed for  $\delta^{13}\text{C}_{\text{org}}$  were from near the base of the well at 2860 m in palynological Stage 3b Zone through to above the Early Triassic/Jurassic unconformity at 1910 m. The  $\delta^{13}\text{C}_{\text{org}}$  of samples analysed from palynological zones Stage 3b, Stage 4 and Lower 5c are consistent around a value of -23‰. Samples in the palynological Upper Stage 5 Zone fluctuated around -25‰. A negative  $\delta^{13}\text{C}_{\text{org}}$  excursion begins in samples from the interval lacking palynological data at 2332 m and continues through the entire palynological *P. microcorpus* Zone to reach its most negative value of -32.65‰ in the *Kraeuselisporites saeptatus* Zone at 2270 m. The  $\delta^{13}\text{C}_{\text{org}}$  negative excursion is marked as the shaded segment B between mean values of -23‰ for the Permian and -32.65‰ for the Early Triassic and occurs over 49 m (assuming it begins at 2319 m) or 61 m (assuming it begins at 2332 m, which is also the base of the Tern Sandstone Member of the Hyland Bay Formation). Following the  $\delta^{13}\text{C}_{\text{org}}$  minimum, values increase to -25.81‰ at 2070 m then decrease to -32.67‰ at 1924 m. The  $\delta^{13}\text{C}_{\text{org}}$  values in the Jurassic Malita Formation above the disconformity are around -24‰. The more negative  $\delta^{13}\text{C}_{\text{org}}$  value of -26.64‰ obtained from a sample from 1839.5 m has a low TOC and is considered unreliable.

The TOC varies erratically throughout the sediments in segment A, declines in segment B and is significantly reduced in segment D. The lithological boundary between the Hyland Bay and Mount Goodwin Formations was placed at 2293.5 m in this well (BHP Petroleum, 1993) and does not coincide with the initiation of the negative  $\delta^{13}\text{C}_{\text{org}}$  excursion or with the base of the *P. microcorpus* Zone.

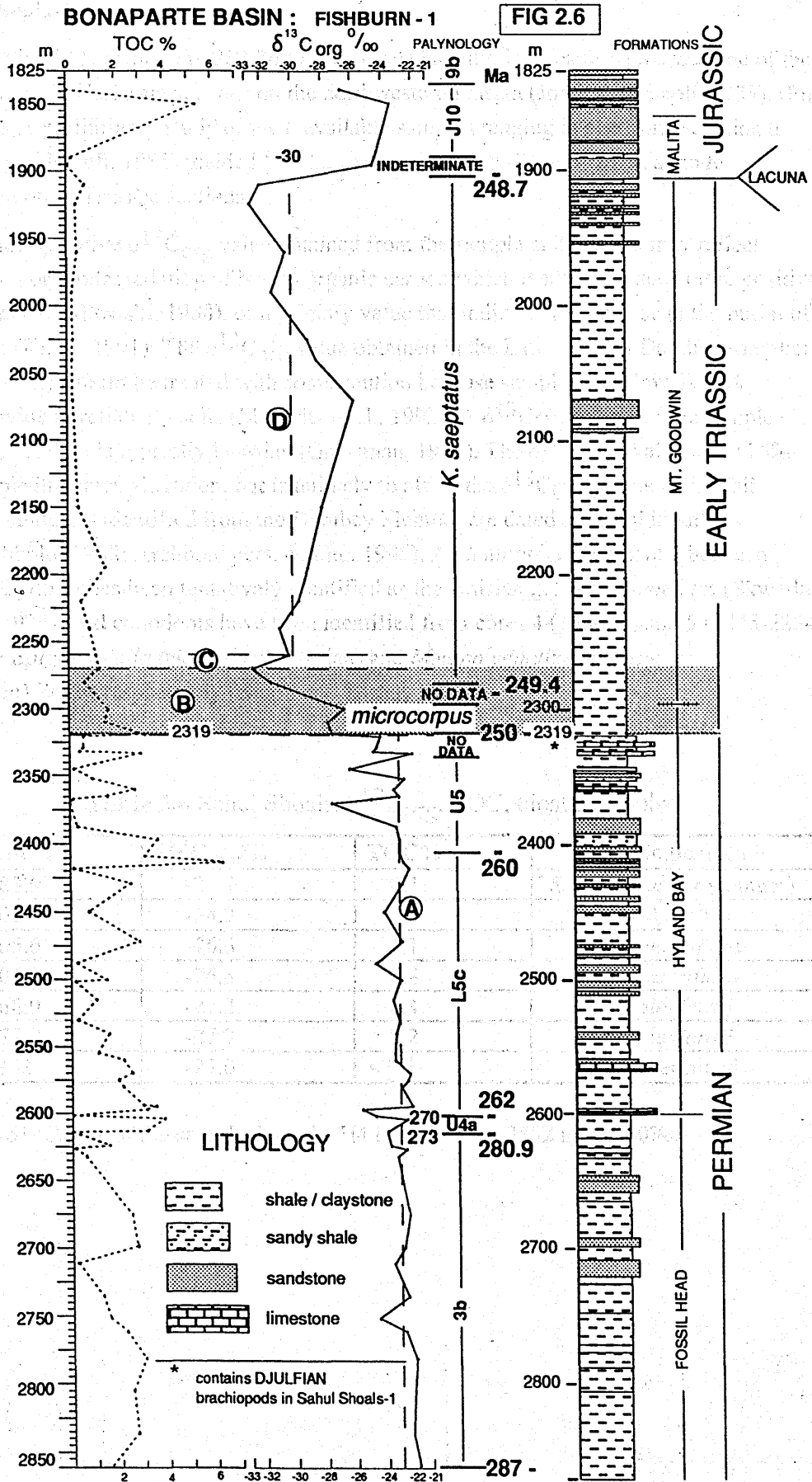
Table 2.5 Fishburn 1.  $\delta^{13}\text{C}_{\text{org}}$ , TOC, biostratigraphy.

Well	depth m	$\delta^{13}\text{C}_{\text{org}} \text{‰}$	TOC%	Palynology Zone
Fishburn 1	1839.5	-26.64	< 0.1	<i>C. torosa</i> (J10)
Fishburn 1	1850	-23.38	5.4	<i>C. torosa</i> (J10)
Fishburn 1	1890	-24.33	0.2	<i>C. torosa</i> (J10)
Fishburn 1	1895.5	-24.53	< 0.1	<i>C. torosa</i> (J10)
Fishburn 1	1910	-32.02	0.8	<i>K. saeptatus</i>
Fishburn 1	1924	-32.67	0.4	<i>K. saeptatus</i>
Fishburn 1	1960	-30.37	0.4	<i>K. saeptatus</i>
Fishburn 1	1990	-31.27	0.2	<i>K. saeptatus</i>
Fishburn 1	2025	-28.95	0.3	<i>K. saeptatus</i>
Fishburn 1	2040	-28.31	0.2	<i>K. saeptatus</i>
Fishburn 1	2070	-25.81	0.2	<i>K. saeptatus</i>
Fishburn 1	2150	-28.02	0.4	<i>K. saeptatus</i>
Fishburn 1	2195	-28.96	1.6	<i>K. saeptatus</i>
Fishburn 1	2220	-29.60	0.5	<i>K. saeptatus</i>
Fishburn 1	2240	-30.88	0.9	<i>K. saeptatus</i>
Fishburn 1	2260	-30.23	1.1	<i>K. saeptatus</i>
Fishburn 1	2270	-32.65	1.3	<i>K. saeptatus</i>
Fishburn 1	2280	-31.47	0.7	<i>K. saeptatus</i>
Fishburn 1	2300	-26.61	1.6	<i>P. microcorpus</i>
Fishburn 1	2310	-27.71	1.5	<i>P. microcorpus</i>
Fishburn 1	2319	-27.41	3.1	<i>P. microcorpus</i>
Fishburn 1	2320.5	-24.24	0.5	Unknown
Fishburn 1	2329	-24.49	0.5	Unknown
Fishburn 1	2332	-24.70	0.4	Unknown
Fishburn 1	2333.5	-22.11	3.0	<i>D. parvithola</i> (U5)
Fishburn 1	2345	-26.29	0.8	<i>D. parvithola</i> (U5)
Fishburn 1	2352	-22.69	0.9	<i>D. parvithola</i> (U5)
Fishburn 1	2360	-23.36	2.71	<i>D. parvithola</i> (U5)
Fishburn 1	2365	-23.05	1.6	<i>D. parvithola</i> (U5)
Fishburn 1	2367	-24.81	0.1	<i>D. parvithola</i> (U5)
Fishburn 1	2370	-27.48	< 0.1	<i>D. parvithola</i> (U5)
Fishburn 1	2387	-23.19	0.3	<i>D. parvithola</i> (U5)
Fishburn 1	2396.6	-22.99	3.6	<i>D. parvithola</i> (U5)
Fishburn 1	2409	-22.90	3.1	<i>D. dulhuntyi</i> (L5c)
Fishburn 1	2413	-22.83	6.3	<i>D. dulhuntyi</i> (L5c)
Fishburn 1	2418	-22.33	0.1	<i>D. dulhuntyi</i> (L5c)
Fishburn 1	2429	-22.80	2.5	<i>D. dulhuntyi</i> (L5c)
Fishburn 1	2450	-24.05	0.8	<i>D. dulhuntyi</i> (L5c)
Fishburn 1	2472	-22.85	2.9	<i>D. dulhuntyi</i> (L5c)
Fishburn 1	2488	-24.61	0.3	<i>D. dulhuntyi</i> (L5c)
Fishburn 1	2500	-22.93	1.5	<i>D. dulhuntyi</i> (L5c)
Fishburn 1	2501.5	-23.06	0.2	<i>D. dulhuntyi</i> (L5c)
Fishburn 1	2515	-23.47	1.1	<i>D. dulhuntyi</i> (L5c)
Fishburn 1	2530	-23.07	0.3	<i>D. dulhuntyi</i> (L5c)
Fishburn 1	2540	-23.29	1.6	<i>D. dulhuntyi</i> (L5c)
Fishburn 1	2555	-23.37	1.1	<i>D. dulhuntyi</i> (L5c)
Fishburn 1	2560	-23.36	2.2	<i>D. dulhuntyi</i> (L5c)

Table 2.5 continued.

Well	depth m	$\delta^{13}\text{C}_{\text{org}} \%$	TOC%	Palynology Zone
Fishburn 1	2570	-22.34	2.5	<i>G. trisinus</i> /young
Fishburn 1	2575	-22.57	1.9	<i>D. dulhuntyi</i> (L5c)
Fishburn 1	2580	-22.93	2.1	<i>D. dulhuntyi</i> (L5c)
Fishburn 1	2594	-22.22	3.0	<i>D. dulhuntyi</i> (L5c)
Fishburn 1	2594.8	-22.28	3.5	<i>D. dulhuntyi</i> (L5c)
Fishburn 1	2597	-25.54	3.1	<i>D. dulhuntyi</i> (L5c)
Fishburn 1	2601.5	-24.69	< 0.1	<i>D. dulhuntyi</i> (L5c)
Fishburn 1	2604	-22.60	3.9	<i>P. sinuosous</i> (U4a)
Fishburn 1	2613	-23.86	3.1	<i>D. villosus</i> (U4b)
Fishburn 1	2614	-23.87	< 0.1	<i>G. trisinus</i> / young (3b)
Fishburn 1	2624	-23.70	1.6	<i>G. trisinus</i> / young (3b)
Fishburn 1	2626	-22.63	0.1	<i>G. trisinus</i> / young (3b)
Fishburn 1	2632	-23.22	0.6	<i>G. trisinus</i> / young (3b)
Fishburn 1	2675	-22.49	2.5	<i>G. trisinus</i> / young (3b)
Fishburn 1	2698	-22.81	2.7	<i>G. trisinus</i> / young (3b)
Fishburn 1	2698.2	-22.81	2.7	<i>P. sinuosus</i> /young (L4)
Fishburn 1	2710.5	-23.51	0.2	<i>G. trisinus</i> / young (3b)
Fishburn 1	2735	-22.58	1.3	<i>G. trisinus</i> / young (3b)
Fishburn 1	2751	-24.52	1.6	<i>G. trisinus</i> / young (3b)
Fishburn 1	2761	-22.76	2.2	<i>G. trisinus</i> / young (3b)
Fishburn 1	2781	-22.05	3.0	<i>G. trisinus</i> / young (3b)
Fishburn 1	2805	-22.22	2.5	<i>G. trisinus</i> / young (3b)
Fishburn 1	2836	-22.32	2.7	<i>G. trisinus</i> / young (3b)
Fishburn 1	2860	-21.87	1.6	<i>G. trisinus</i> / young (3b)

**Figure 2.6** Fishburn 1, Bonaparte Basin, northwestern Australia. Total organic carbon (TOC),  $\delta^{13}\text{C}_{\text{org}}$ , palynological zones (R.J. Helby, unpublished Palynology Report to BHP Petroleum, 1993), lithological log and formations (BHP Petroleum, 1993). The dotted line at 2319 m is my pick of the Permian-Triassic boundary. An alternative pick would place the Permian-Triassic boundary at the base of the Tern Sandstone member at 2332 m. The sediments in and about the interval of the negative  $\delta^{13}\text{C}_{\text{org}}$  isotope excursion are interpreted to have been deposited in a marine environment (B.J. Messent pers. comm., 1993).



2.1.4 Sahul Shoals-1

Sahul Shoals-1, drilled in 1969-70 to investigate an anticlinal feature, provides one of the most complete marine Triassic sections on the northwestern margin (Jones and Nicoll, 1985), (Fig. 2.7, Table 2.6). A preliminary study of the 6 available samples ranging in age from Scythian to Norian (Jones and Nicoll, 1985) yielded  $\delta^{13}\text{C}_{\text{org}}$  values between -24 and -28‰, a range encompassed in other Triassic sections.

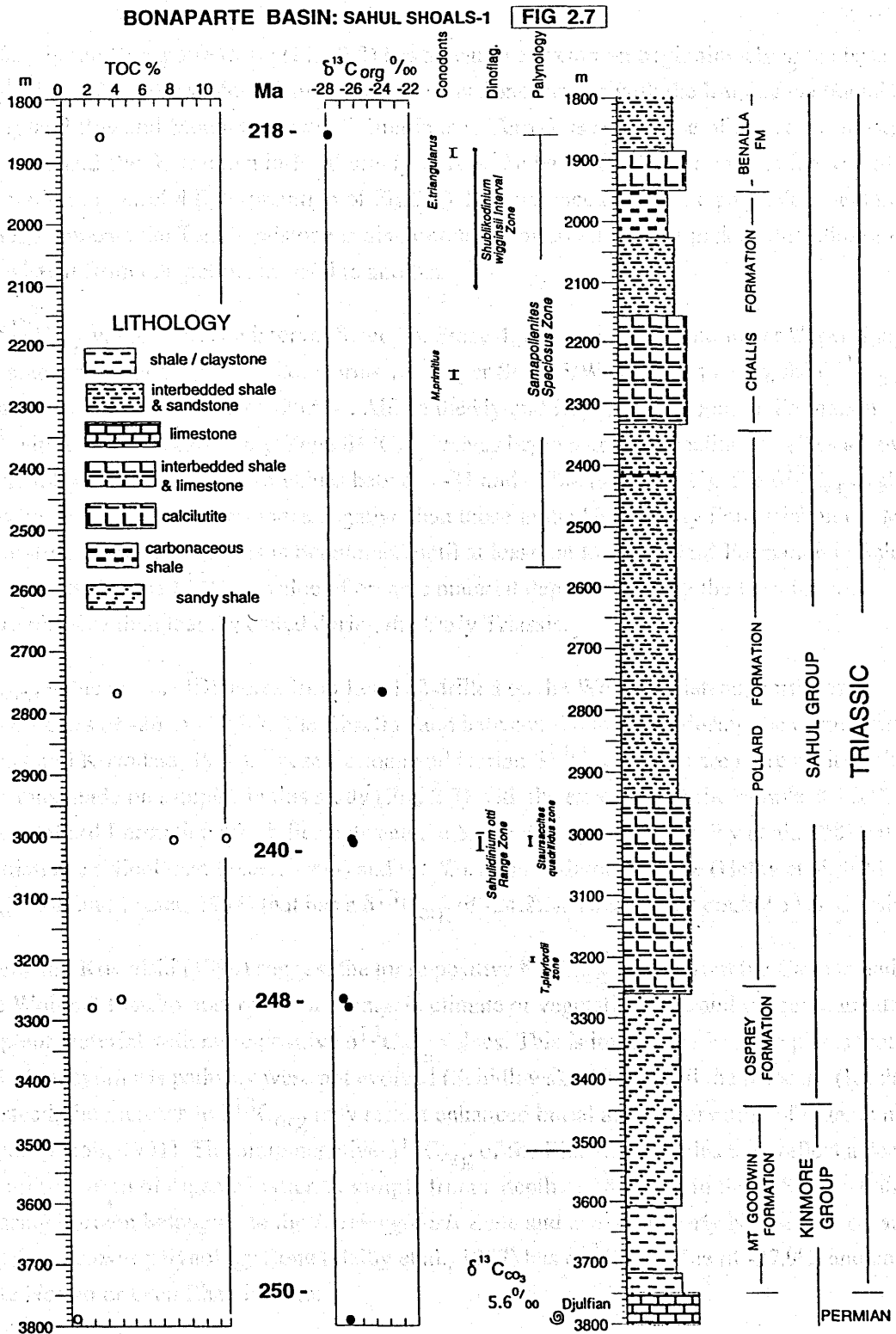
The more positive  $\delta^{13}\text{C}_{\text{org}}$  value obtained from the sample at 2769.8 m may reflect partial oxidation or biodegradation of buried organic carbon which tends to produce more positive  $\delta^{13}\text{C}_{\text{org}}$  values (Schidlowski, 1988), or a primary value that indicates an increase in the burial of organic carbon (Knoll, 1991). The  $\delta^{13}\text{C}_{\text{org}}$  value obtained in the Late Permian Dombey Member limestone (3802 m) should be treated with some caution because samples with low TOC% commonly provide unreliable results (Magaritz et al., 1992). A  $\delta^{13}\text{C}_{\text{CO}_3}$  value of the sample from 3802 m of 5.60‰ is typically Permian (Grossman, 1994). The  $\delta^{18}\text{O}_{\text{CO}_3}$  value of -9.28‰ from that sample indicates alteration, but is unlikely to affect the  $\delta^{13}\text{C}_{\text{CO}_3}$  value (Marshall, 1992). The brachiopods identified from the Dombey Member are dated as "Chhidruan" (= Djulfian) (Archbold, 1988; Archbold pers. comm., 1995). An ammonite from core 9 between 3272.35 and 3267.5 m has been tentatively identified as the Anisian genus, *Nicomedites* (Skwarko and Kummel, 1974), and conodonts have been identified from cores 4 (1886 m) and 5 (2245-2254 m) as from the *Epigondolella triangularis* (Norian) and *Metapolygnathus primitus* (Carnian/Norian) Zones respectively (Nicoll and Foster, 1994).

Table 2.6 Sahul Shoals.  $\delta^{13}\text{C}_{\text{org}}$ , TOC, biostratigraphy.

Depth m	$\delta^{13}\text{C}_{\text{org}}\text{‰}$	TOC%	Palynological Zone
1883.9	-27.9	0.3	<i>S. speciosus</i> (or younger)
2769.8	-24.2	0.4	undetermined
3005.6	-26.6	1.1	<i>S. quadrifidus</i>
3005.9	-26.5	0.8	<i>S. quadrifidus</i>
3268.9	-27.2	0.4	<i>T. playfordii</i>
3272.9	-27.0	0.2	<i>T. playfordii</i>
3802	-27.0	< 0.1	undetermined

$\delta^{13}\text{C}_{\text{CO}_3}$  of the sample from the H4 Limestone at 3802 m is 5.60‰.





**Figure 2.7** Sahul Shoals-1, Bonaparte Basin, northwestern Australia. Total organic carbon (TOC),  $\delta^{13}C_{org}$ , palynological zones (Helby et al., 1987), dinoflagellate zones (Helby et al., 1987), conodont zones (Nicoll and Foster, 1994), lithological log, and formations (BOCAL, 1970).  $\delta^{13}C_{org}$  has a mean value of about -27‰ for the latest Permian and Early to Late Triassic. The  $\delta^{13}C_{CO_3}$  value of 5.60‰ (asterisk) is plotted at the  $\Delta$  offset of about -27‰.

### 2.1.5 Bonaparte Basin synopsis

$\delta^{13}\text{C}_{\text{org}}$  in the Bonaparte Basin (Fig. 2.8) has a negative excursion beginning about the base of the palynological *P. microcorpus* Zone. This negative excursion coincides with the lithological boundary between the Hyland Bay and Mount Goodwin Formations in Tern-3, is at the base of the Tern Sandstone Member of the Hyland Bay Formation in Fishburn-1 but is in the base of the basal units of the Mount Goodwin Formation in Petrel-4 (interpretation of Fig 2.4). By reference to both the palynology and the  $\delta^{13}\text{C}_{\text{org}}$  values it appears the Tern Sandstone is diachronous or alternatively the pick of this lithological unit is not consistent from one petroleum well to another.

The  $\delta^{13}\text{C}_{\text{org}}$  values over the interval Stage 3b, Stage 4, Lower Stage 5, and lower Upper Stage 5 are relatively stable at around -22 to -24‰. During the Upper Stage 5/Weylandites zones, the  $\delta^{13}\text{C}_{\text{org}}$  values fluctuate over the range -22.5 to -26.9‰. Above the Hyland Bay/Mount Goodwin Formation boundary and within the *P. microcorpus* Zone  $\delta^{13}\text{C}_{\text{org}}$  values begin a gradual decline to values as low as -34.5‰ (segment B) before returning to values between -31 and -27‰ (segment C). The  $\delta^{13}\text{C}_{\text{org}}$  values then appear to be maintained at levels more negative than those in the Hyland Bay Formation in the Mount Goodwin Formation (segment D). This is maintained until at least the lower Pollard Formation in Sahul Shoal-1 and suggests that the  $\delta^{13}\text{C}_{\text{org}}$  value of organic material deposited during the Permian was generally more positive than that deposited during the Early Triassic.

$\delta^{13}\text{C}_{\text{org}}$  values from ODP cores from Leg 122 drilled on the Wombat Plateau, northwest Australia, have values of -26 to -27‰ in the Rhaetian and between -20 to -26‰ during the Carnian and Norian (Meyers and Kowalski, 1994). These Carnian and Norian  $\delta^{13}\text{C}_{\text{org}}$  values are more positive than the determinations made on samples in this study (Fig. 2.7) with the exception of the sample at 2769.8 m from the upper Pollard Formation which lies between the *S. otti* dinocyst Zone (Helby et al., 1987) of Anisian/Ladinian age (Nicoll and Foster, 1994) and the *S. wigginsii* dinocyst Zone (Helby et al., 1987) of Carnian age (Nicoll and Foster, 1994) that has a  $\delta^{13}\text{C}_{\text{org}}$  of -24.2‰. This sample could be late Carnian.

Meyers and Kowalski (1994) suggest the more positive  $\delta^{13}\text{C}_{\text{org}}$  values from the Carnian and Norian of the Wombat Plateau may reflect a change in climate or vegetation type and suggest a greater influx of C4 plant material with more positive  $\delta^{13}\text{C}_{\text{org}}$  values. This is impossible because plants that utilise the C4 photosynthesis pathway were not evolved (Schidlowski, 1988) until the Miocene (Koch et al., 1992). Instead, the increase in  $\delta^{13}\text{C}_{\text{org}}$  may reflect enhanced burial and preservation of organic matter during this time (Knoll, 1991). The more negative  $\delta^{13}\text{C}_{\text{org}}$  of the Rhaetian samples may reflect a decline in burial and preservation of organic matter. A sample from a depth of 1883.9 m in Sahul Shoals-1 above a conodont-bearing horizon belonging to the *E. triangularis* Zone and above the early Norian (Nicoll and Foster, 1994) *S. speciosus* palynology Zone (Helby et al., 1987) has  $\delta^{13}\text{C}_{\text{org}}$  value of -27.9‰ and could be of very late Norian or even Rhaetian age.

The  $\delta^{13}\text{C}_{\text{org}}$  values from Middle and Late Triassic Sahul Shoals-1 samples (Fig. 2.7) are similar to those of Wombat Plateau ODP leg 122 (Meyers and Kowalski, 1994). The assertion by Morante et al. (1994) that the  $\delta^{13}\text{C}_{\text{org}}$  of -24.2‰ from 2769.8 m in Sahul Shoals-1 did not reflect a primary value is therefore not supported by the new data (Meyers and Kowalski, 1994) from the Carnian and could indicate that  $\delta^{13}\text{C}_{\text{org}}$  values during the Carnian were similar to the Late Permian. Interestingly, Simms and Ruffel (1989) recognise a Carnian/Norian boundary climate change and a major faunal and floral turnover. The apparent, but poorly constrained negative excursion in  $\delta^{13}\text{C}_{\text{org}}$  between the Carnian and Rhaetian of the

northwest of Australia suggested by the data from Sahul Shoals-1 and the ODP Leg 122 (Meyers and Kowalski, 1994) may be associated with the late Carnian extinction and is a possible avenue for future chemostratigraphic study.

Table 2.7 Summary of the stratigraphy and sedimentation rates (modified from Krieger, 1994)

Table 2.7 Summary of the stratigraphy and sedimentation rates (modified from Krieger, 1994)

Table 2.7 Summary of the stratigraphy and sedimentation rates (modified from Krieger, 1994)

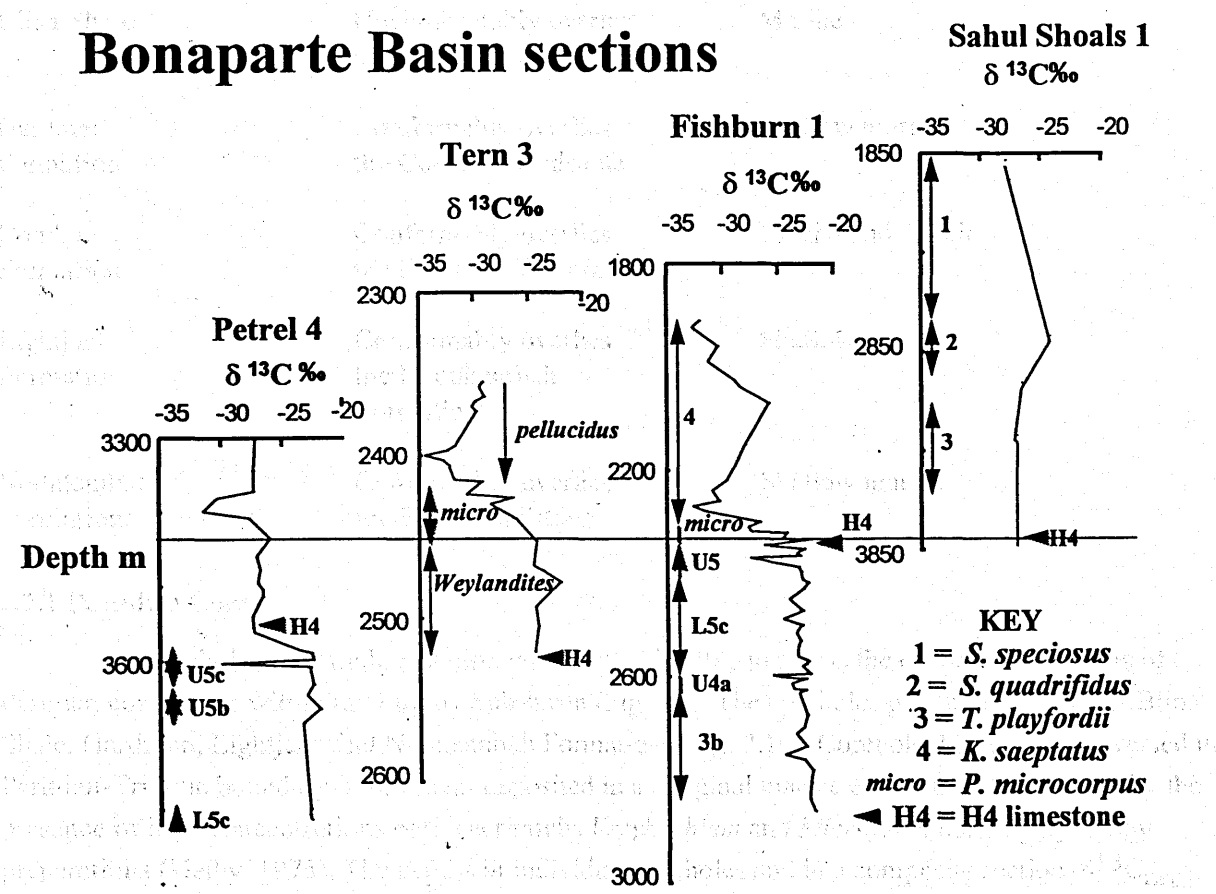


**Figure 2.8** Bonaparte Basin  $\delta^{13}\text{C}_{\text{org}}$  profiles aligned on the beginning of the  $\delta^{13}\text{C}_{\text{org}}$  excursion (solid line). The key lithological marker, the H4 Limestone (= Dombey Member) and known palynological zone ranges are shown.

Determination of the depth of the lowermost Dombey Member is uncertain due to the position of the base of the section. The depth of the base of the section (Dombey) is 229.5 m in the composite section (Fig. 2.10).

Between 229.5 m and 229 m in the composite section, at the Dombey Member (Dombey) section,  $\delta^{13}\text{C}_{\text{org}}$  values decrease from around -20‰ to -33‰ (Fig. 2.10) in sediments. A sample of the *P. saeptatus* zone at 229 m (Dombey) section (Fig. 2.10) shows the  $\delta^{13}\text{C}_{\text{org}}$  excursion is also compared to that in the Fishburn and Sahul Shoals (Fig. 2.8, 2.9) consistent with an interpretation of a condensed section or hiatus at the Permian-Triassic boundary.

## 2.2 Canning Basin

The Canning Basin is on and offshore in its areal extent. The basin contains sediments from Ordovician to Holocene in age. The present study concentrates on Permian and Triassic sediments deposited in the Fitzroy Trough. The stratigraphy and environment of deposition of units in the interval studied are summarised in Table 2.7.

**Table 2.7** Canning Basin stratigraphy and depositional environments modified from Middleton (1990).

Unit	Stratigraphic relationships	Depositional environment
Blina Shale	Unconformably overlies the Hardman Formation	Marine
Hardman Formation	Conformably overlies the Condren Sandstone	Shallow marine
Condren Formation	Conformably overlies the Lightjack Formation	Fluvial and deltaic
Lightjack Formation	Conformably overlies the Noonkambah Formation	Shallow marine
Noonkambah Formation	Conformably overlies the Poole Sandstone	Shallow marine

### 2.2.1 Paradise Cores

Six coreholes on Paradise Station were drilled in 1971 to assess the economic prospects of Permian coal seams within the Fitzroy Sub-basin (Fig. 2.9). The coreholes penetrated the lower Blina Shale, Hardman, Lightjack and Noonkambah Formations (Fig. 2.10). Corehole 4 (Fig 2.11) traversed the Permian-Triassic boundary in sediment deposited in a marginal marine environment, indicated by the presence of high concentrations of the acritarchs *Veryhachium* and *Micrhystridium* in palynology preparations (Helby, 1975). The depths in individual coreholes and in a composite section,  $\delta^{13}\text{C}_{\text{org}}$  values, TOC and biostratigraphical assignment of samples from this section are listed in Table 2.8 and the new biostratigraphic zonation about the  $\delta^{13}\text{C}_{\text{org}}$  excursion is listed in Table 2.9 (R.J. Helby pers. comm., 1993, 1994).

Determination of the depth of the lowermost Blina Shale is uncertain but based on the description of the basal transgressive sandstone of this formation (Gorter, 1978) it is placed at 229.5 m in the composite section (Fig. 2.10).

Between 229.5 m and 229 m in the composite section, at the Hardman Formation/ Blina Shale boundary,  $\delta^{13}\text{C}_{\text{org}}$  values change from around -26‰ to -33‰ (Fig. 2.10) in sediments straddling a sample of the *P. microcorpus* Zone at 229 m (Helby, pers. comm., 1993). The  $\delta^{13}\text{C}_{\text{org}}$  excursion is sharp compared to that in the Tern-3 and Fishburn-1 wells (Figs 2.3, 2.6), consistent with an interpretation of a condensed section or lacuna at the Permian-Triassic boundary.

The H/C (hydrogen/carbon) ratio of kerogen from a sample below the  $\delta^{13}\text{C}_{\text{org}}$  excursion at a composite depth of 229.54 m is 1.43 and from a sample above the excursion (220.38 m) is 1.31. If kerogen from rocks less than 1.6 Ga have H/C greater than 0.3 then the primary  $\delta^{13}\text{C}_{\text{org}}$  signal is probably preserved (Hayes et al, 1983). The  $\delta^{13}\text{C}_{\text{org}}$  obtained on the kerogens for these two samples was less than the standard deviation determined on 48 analyses of a laboratory standard (0.13‰) (see Appendix 2.2, Fig. 38) when compared to the values obtained from the whole-rock TOC in the same samples.

Sm/Nd (samarium/neodymium) model ages of sediments below and above the  $\delta^{13}\text{C}_{\text{org}}$  excursion were determined to see if there was any evidence of a change in sediment provenance about the interval of the  $\delta^{13}\text{C}_{\text{org}}$  excursion. The results are listed in Table 2.10 and a description of the analysis technique is in Appendix 2.3.

Because the Sm/Nd ratio is largely unaffected by intracrustal processes, a model age can be determined that indicates when the Nd departed from the mantle. Detrital sediments are formed from reworked crustal material and inherit the average Sm/Nd crustal age of the sediment sources (Chaudhuri et al., 1992) hence the model age has no direct applicability to the age of deposition. However, a change in the Sm/Nd model age of sediments indicates a change in the overall composition of the sediment (Mearns et al., 1988). In the Paradise # 4 core, Sm/Nd model ages determined on pelites (Table 2.10) increase towards the negative  $\delta^{13}\text{C}_{\text{org}}$  excursion from values of 1.692 Ga at 105.77 m (347 feet) to 2.023 Ga at 90.53 m (297 feet), and 2.250 Ga at 87.48 m (287 feet). By 69.19 m (227 feet) the model age decreased to 1.963 Ga. The trend suggests a change in sediment provenance through this interval.

This change in the Sm/Nd model age takes place in the interval of most rapid  $\delta^{13}\text{C}_{\text{org}}$  change, and supports an interpretation of an hiatus between samples during which the sediment provenance changed. An explanation for this change is replacement of the dense Upper Stage 5 palynological zone megaflora by the sparse *L. pellucidus* Zone megaflora and concomitant accelerated erosion of uplands. Alternatively, Balme (1969, p. 111) suggested that the lowermost Triassic palynomorphs in sediments in the marine Perth, Carnarvon and Canning Basins represent "specialised coastal plant communities" which may reflect a loss of flora and hence a change in the pattern of erosion and sediment provenance. A further possibility is that the Sm/Nd model ages reflect a changing erosion pattern associated with the regressive-transgressive Permian-Triassic boundary (Holser and Magaritz, 1987).

The TOC of samples above the  $\delta^{13}\text{C}_{\text{org}}$  excursion is markedly lower (< 0.5%) than those from below the  $\delta^{13}\text{C}_{\text{org}}$  excursion (commonly 2 to 3 %). This reflects a decline in the proportion of organic matter preserved in sediments above the negative  $\delta^{13}\text{C}_{\text{org}}$  excursion in the Canning Basin. Possible causes of this are:

- a) lower primary production by extinction,
- b) less preservation of organic matter due to increased oxidation although this would seem unlikely as the most common macro-fossils preserved in the lower Blina Shale in these coreholes are the brachiopod *Lingula*, thought to be adapted to low oxygen environments, or
- c) both lower productivity and increased oxidation. This is discussed more fully in Chapter 6.

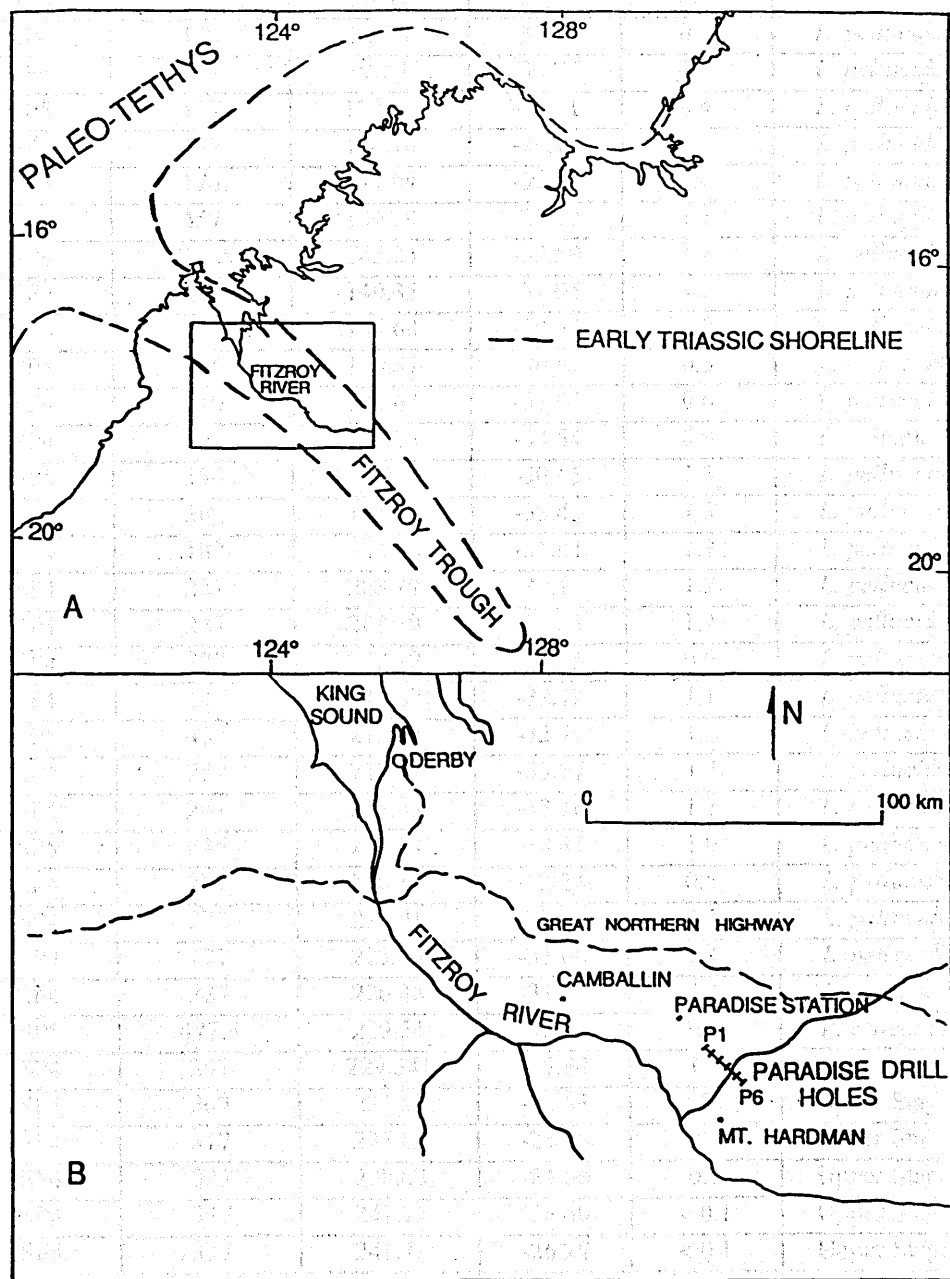


**Figure 2.9** Location of the Paradise Coreholes (P1- P6). The position of the Early Triassic shoreline is from Veevers et al. (1984, fig. 240).

Table 2.8 Paradise Coreholes 1-6,  $\delta^{13}\text{C}_{\text{org}}$ , TOC, and biostratigraphy.

Drill Hole	Depth Ft	Depth m comp	$\delta^{13}\text{C}_{\text{org}}\%$	TOC%	Palynology Zone
SP6	77	23.47	-31.17	0.4	
SP6	116	35.35	-31.17	0.7	<i>L. pellucidus</i>
SP6	317	96.62	-30.75	0.6	<i>L. pellucidus</i>
SP5	127	122.71	-30.51	0.4	<i>L. pellucidus</i>
SP5	137	125.76	-28.71	0.6	<i>L. pellucidus</i>
SP5	174	137.04	-31.20	0.8	<i>L. pellucidus</i>
SP6	457	139.29	-32.92	1.1	<i>L. pellucidus</i>
SP6	476.5	145.24	-32.59	1.1	<i>L. pellucidus</i>
SP6	490	149.35	-32.95	1.2	<i>L. pellucidus</i>
SP4	58	156.68	-30.94	1.0	<i>L. pellucidus</i>
SP5	285	170.87	-30.92	0.5	<i>L. pellucidus</i>
SP4	110	172.63	-32.63	0.6	<i>L. pellucidus</i>
SP4	132	179.23	-34.54	0.9	<i>L. pellucidus</i>
SP5	356	192.2	-30.85	1.3	<i>L. pellucidus</i>
SP5	362	194.34	-33.43	1.3	<i>L. pellucidus</i>
SP4	187	196	-31.91	1.9	<i>L. pellucidus</i>
SP4	227	208.19	-33.13	1.2	<i>L. pellucidus</i>
SP4	227	208.19	-32.63	1.2	<i>L. pellucidus</i>
SP4	227	208.19	-34.45	0.9	<i>L. pellucidus</i>
SP4	247	214.29	-32.72	1.1	<i>L. pellucidus</i>
SP5	435	216.59	-32.78	1.3	<i>L. pellucidus</i>
SP4	257	217.33	-33.07	1.7	<i>L. pellucidus</i>
SP4	261	218.55	-33.16	1.3	<i>L. pellucidus</i>
SP5	445	219.64	-30.31	1.0	<i>L. pellucidus</i>
SP4	267	220.38	-32.24	0.5	<i>L. pellucidus</i>
SP4	272	221.91	-32.83	1.1	<i>L. pellucidus</i>
SP4	277	223.43	-33.00	1.4	<i>L. pellucidus</i>
SP4	287	226.48	-33.15	2.4	<i>L. pellucidus</i>
SP5	477.5	229.54	-32.50	0.9	<i>P. reticulatus</i>
SP4	297	229.541	-25.84	1.9	<i>P. microcorpus</i>
SP4	307	232.57	-24.65	< 0.1	Upper Stage 5
SP4	317	235.62	-24.78	7.7	Upper Stage 5
SP4	327	238.67	-24.66	0.7	Upper Stage 5
SP4	337	241.72	-26.60	< 0.1	Upper Stage 5
SP4	337	241.72	-26.28	< 0.1	Upper Stage 5
SP4	347	244.77	-23.88	4.6	Upper Stage 5
SP4	357	247.81	-24.22	3.2	Upper Stage 5
SP4	367	250.86	-23.84	3.7	Upper Stage 5
SP4	377	253.91	-23.95	2.4	Upper Stage 5
SP4	387	256.96	-23.78	2.6	Upper Stage 5
SP4	420	267.02	-23.85	2.4	Upper Stage 5
SP4	437	272.2	-23.06	3.3	Upper Stage 5
SP4	457	278.29	-23.12	2.7	Upper Stage 5
SP4	497	290.49	-23.44	0.5	Upper Stage 5
SP4	537	302.68	-24.00	1.1	Upper Stage 5
SP4	547	305.73	-23.80	1.3	Upper Stage 5
SP4	577	314.87	-23.06	1.0	Upper Stage 5
SP4	609	324.62	-22.68	6.8	Upper Stage 5
SP4	647	336.21	-22.99	1.5	Upper Stage 5

Drill Hole	Depth Ft	Depth m comp	$\delta^{13}\text{Corg}\%$	TOC%	Palynology Zone
SP4	679.5	346.11	-22.51	4.0	Upper Stage 5
SP4	687	348.39	-22.76	< 0.1	Upper Stage 5
SP3	82	349.99	-23.42	0.8	Upper Stage 5
SP4	707	354.49	-22.40	1.7	Upper Stage 5
SP3	327	424.67	-22.75	3.4	Upper Stage 5
SP3	381	441.13	-22.66	3.1	Upper Stage 5
SP3	452.5	462.92	-22.63	9.6	Upper Stage 5
SP3	467	467.34	-22.90	3.6	Upper Stage 5
SP3	505	478.92	-22.25	5.4	Upper Stage 5
SP3	564.5	497.06	-23.61	6.7	Upper Stage 5
SP3	564.5	497.06	-23.82	6.7	Upper Stage 5
SP3	590	504.83	-23.00	4.6	Upper Stage 5
SP3	590	504.83	-22.94	4.6	Upper Stage 5
SP3	610.5	511.08	-22.66	7.1	Upper Stage 5
SP3	610.5	511.08	-22.82	7.1	Upper Stage 5
SP3	625	515.5	-22.73	4.6	Upper Stage 5
SP3	625	515.5	-22.65	4.6	Upper Stage 5
SP3(2)	555	585.16	-23.78	5.2	Upper Stage 5
SP3(2)	608	601.32	-22.99	6.5	Upper Stage 5
SP3(2)	608	601.32	-22.83	6.5	Upper Stage 5
SP3(2)	653	615.03	-22.94	4.6	Upper Stage 5
SP3(2)	653	615.03	-22.91	4.6	Upper Stage 5
SP3(2)	751	644.9	-22.89	5.8	Upper Stage 5
SP3(2)	777.5	652.98	-22.63	5.1	Upper Stage 5
SP3(2)	777.5	652.98	-22.60	5.1	Upper Stage 5
SP3(2)	804.5	661.21	-22.66	4.9	Upper Stage 5
SP2	227	696.19	-22.63	4.8	Upper Stage 5
SP3(2)	950	705.56	-22.52	4.6	Lower Stage 5
SP3(2)	968	711.05	-22.35	4.5	Lower Stage 5
SP2	293	716.31	-22.51	4.5	Lower Stage 5
SP2	324	725.26	-22.30	1.0	Lower Stage 5
SP2	333	728.5	-21.99	1.0	Lower Stage 5
SP2	376.5	741.76	-22.63	1.3	Lower Stage 5
SP1	77	747.47	-22.38	36	Lower Stage 5
SP2	397	748.01	-22.17	0.5	Lower Stage 5
SP2	407	751.05	-21.88	0.5	Lower Stage 5
SP1	94	752.65	-22.05	5.6	Lower Stage 5
SP2	423	755.93	-22.09	2.9	Lower Stage 5
SP2	436.5	760.05	-22.17	4.7	Lower Stage 5
SP2	457	766.29	-21.61	3.5	Lower Stage 5
SP2	462	767.82	-21.80	4.6	Lower Stage 5
SP2	515	786.11	-22.44	7.0	Upper Stage 4b
SP2	522	786.11	-22.42	8.3	Upper Stage 4b
SP2	565	799.21	-22.16	6.6	Upper Stage 4b
SP1	277	808.43	-25.06	4.2	Upper Stage 4b
SP2	597	808.97	-24.82	4.5	Upper Stage 4b
SP2	611	813.23	-24.36	3.8	Upper Stage 4b
SP1	835	978.51	-22.45	3.4	Lower Stage 4
SP1	1070	1045.87	-22.92	3.4	Lower Stage 4



Table 2.9 Palynological determinations by R. J. Helby (pers. comm. 1993; 1994) of Paradise #4 samples.

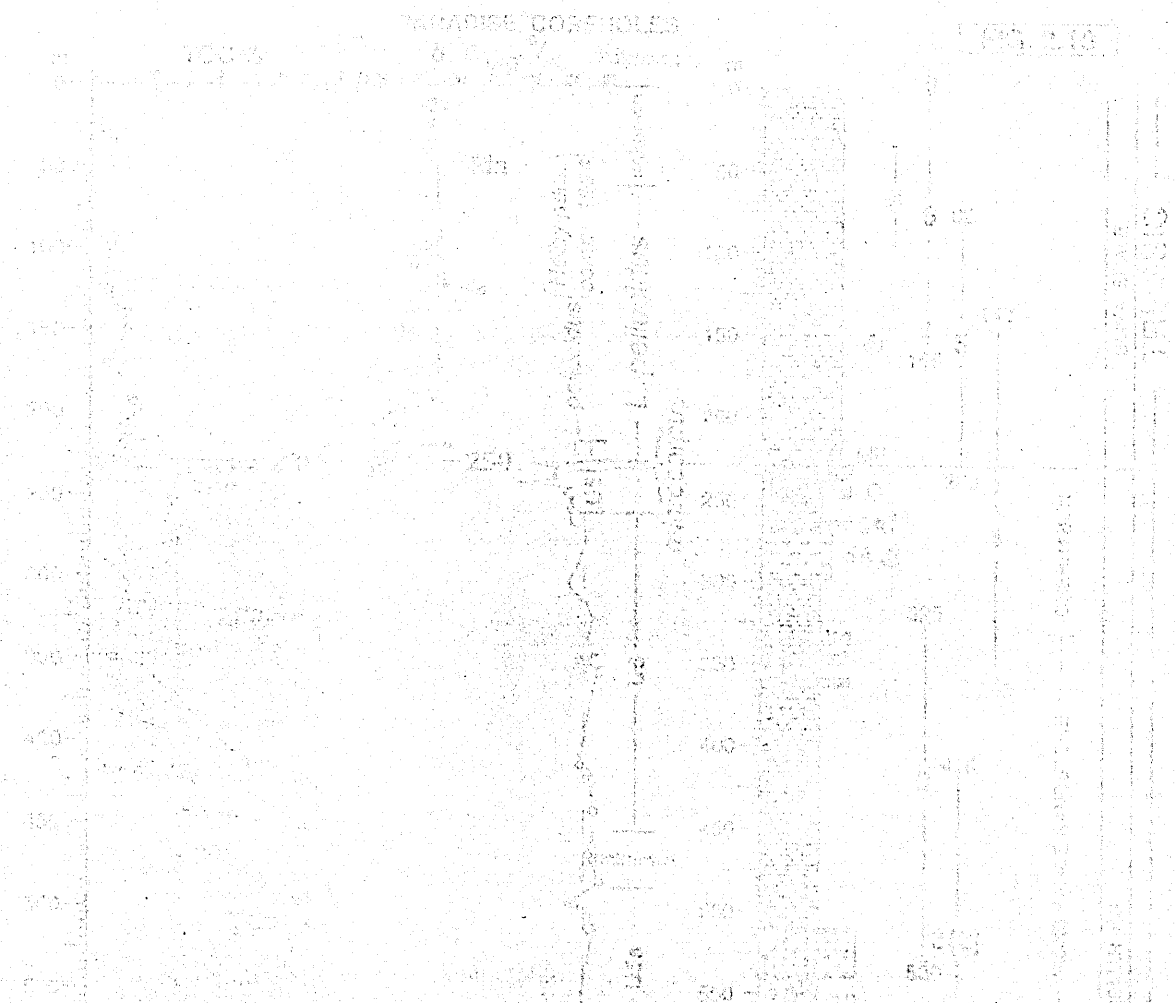
Depth (feet)	Depth (metres)	Zone
257	78.33	<i>L. pellucidus</i>
267	81.38	<i>L. pellucidus</i>
272	82.90	<i>L. pellucidus</i>
277	84.43	<i>L. pellucidus</i>
287	87.5	<i>L. pellucidus</i>
297	90.53	<i>P. microcorpus</i>
317	96.62	Upper stage 5
347	105.77	Upper stage 5
367	111.86	Upper stage 5
387*	117.96	Upper stage 5

\* Supersedes determination of *P. reticulatus* by Paten and Price in Crowe et al. (1978, enclosure 1). The other determination of *P. reticulatus* at 128 m, in #4 by Paten and Price figured in Crowe et al. 1978, likewise conflicts with the determination of Upper Stage 5 by Helby (1975).

Table 2.10 Sm/Nd model ages of fine-grained sediments about the  $\delta^{13}\text{C}_{\text{org}}$  isotope excursion.

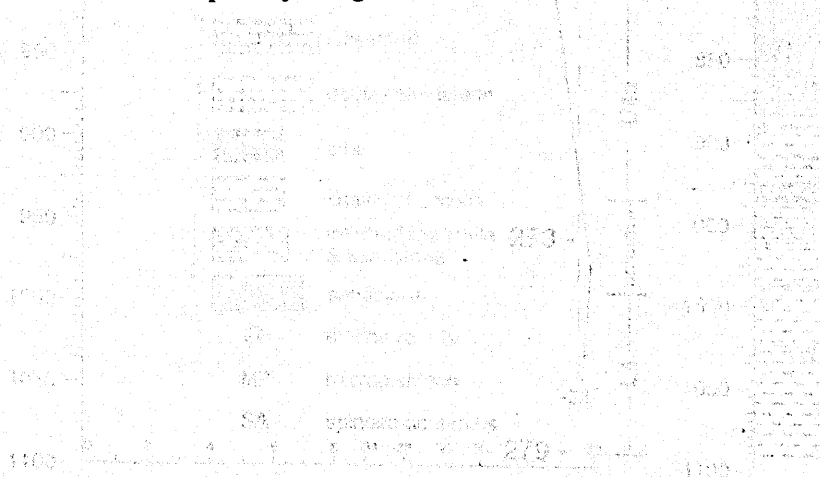
COREHOLE	DEPTH /FEET corehole	DEPTH m composite section	$^{143}\text{Nd}/^{144}\text{Nd}$	$^{147}\text{Sm}/^{144}\text{Nd}$	Model Age DM (DePaolo) Ga
SP4	227	208.19	0.511863	0.1221	1.963
SP4	272	221.91	0.511826	0.1252	2.098
SP4	287	226.48	0.511913	0.1369	2.25
SP4	297	229.541	0.511872	0.1254	2.023
SP4	317	235.62	0.512003	0.1293	1.876
SP4	327	238.67	0.512139	0.1414	1.904
SP4	337	241.72	0.511821	0.1097	1.788
SP4	347	244.77	0.51204	0.1235	1.692

Standard deviation  $^{147}\text{Sm}/^{144}\text{Nd}$  is 0.1%; two standard deviations determined on the standard O'Nions Nd for 20 ratios throughout the time interval over which these analyses were conducted was 0.0026%. Depleted mantle (DM) model ages calculated following the model of DePaolo (1981). From the analytical uncertainties the precision on model ages is  $\pm 50$  Ma (Whitford et al., 1994).



**Figure 2.10** Composite section of Paradise core-holes 1-6, Fitzroy Trough, northern Canning Basin, northwestern Australia showing total organic carbon (TOC),  $\delta^{13}\text{C}_{\text{org}}$ . Palynological zones from Crowe et al. (1978), originally determined by R. Helby. The Permian section was revised by R. Paten and P. Price and expressed in the terminology of Price (1983); subsequently R. Helby (pers. comm. 1993, 1994) has made additional determinations on material from core-hole 4 (Table 2.9). Lithological log, formations, and correlations of individual coreholes are from Crowe et al., (1978). I have amended the correlation of #4 in respect to #3 and #5, because a)  $\delta^{13}\text{C}_{\text{org}}$  is  $< -30\text{‰}$  at and above a depth of 87.48 m in #4 (Fig. 2.11), and at and above a depth of 145.4 m in #5, and b) samples contain *P. microcorpus* at 90.53 m in #4 (R. Helby pers. comm. 1993) and, called the synonymous *P. reticulatus*, at 147.83 m in #5 (Helby, 1975)

This interpretation supersedes the interpretation of lithological correlations, interpolated palynological zones, and placement of the Permian-Triassic boundary based on less complete information in Morante (1993). Samples circled about the  $\delta^{13}\text{C}_{\text{org}}$  excursion are from cores # 3, 5, and 6. Uncircled samples about the  $\delta^{13}\text{C}_{\text{org}}$  excursion are from core-hole 4 shown separately in Fig. 2.11.



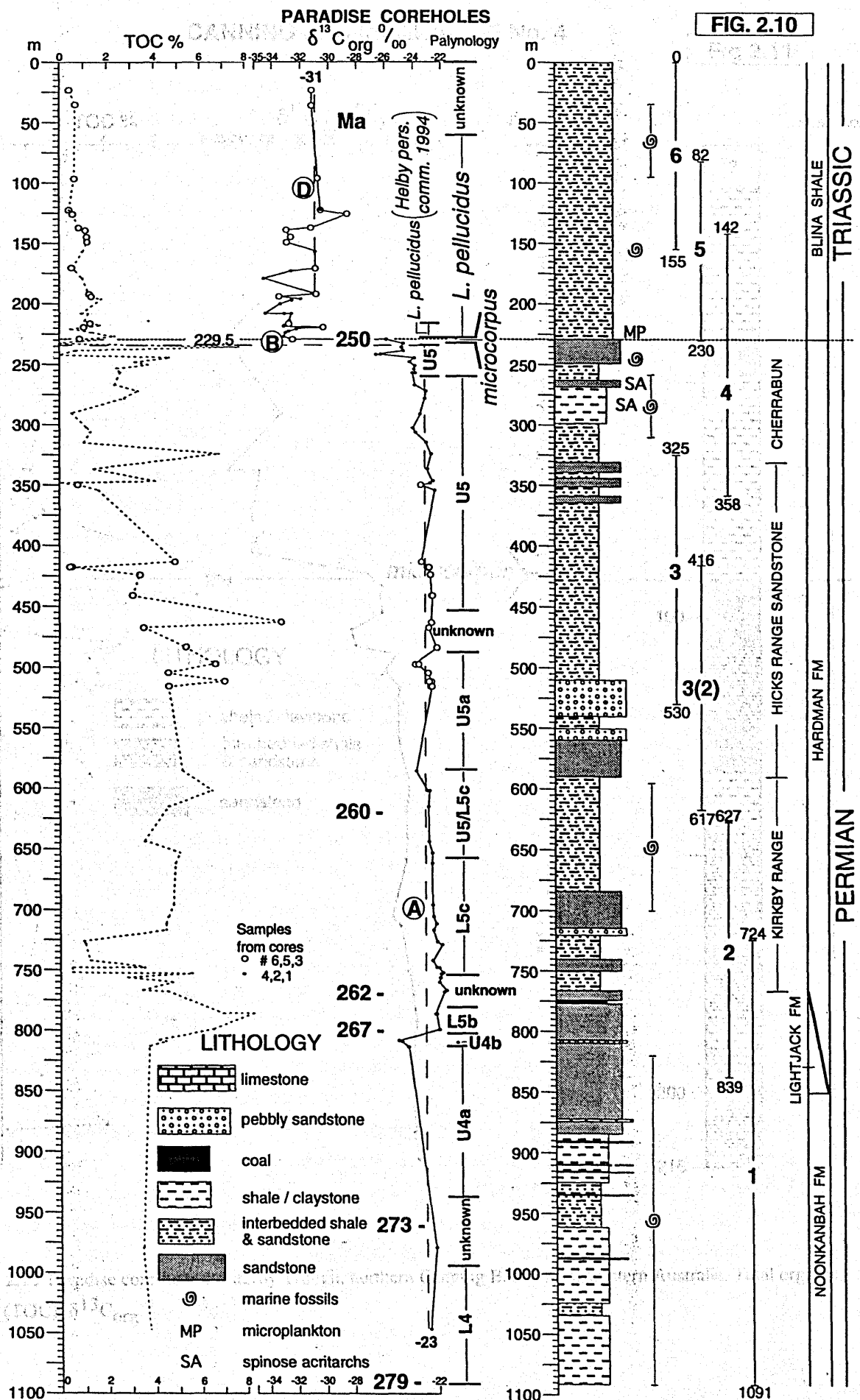
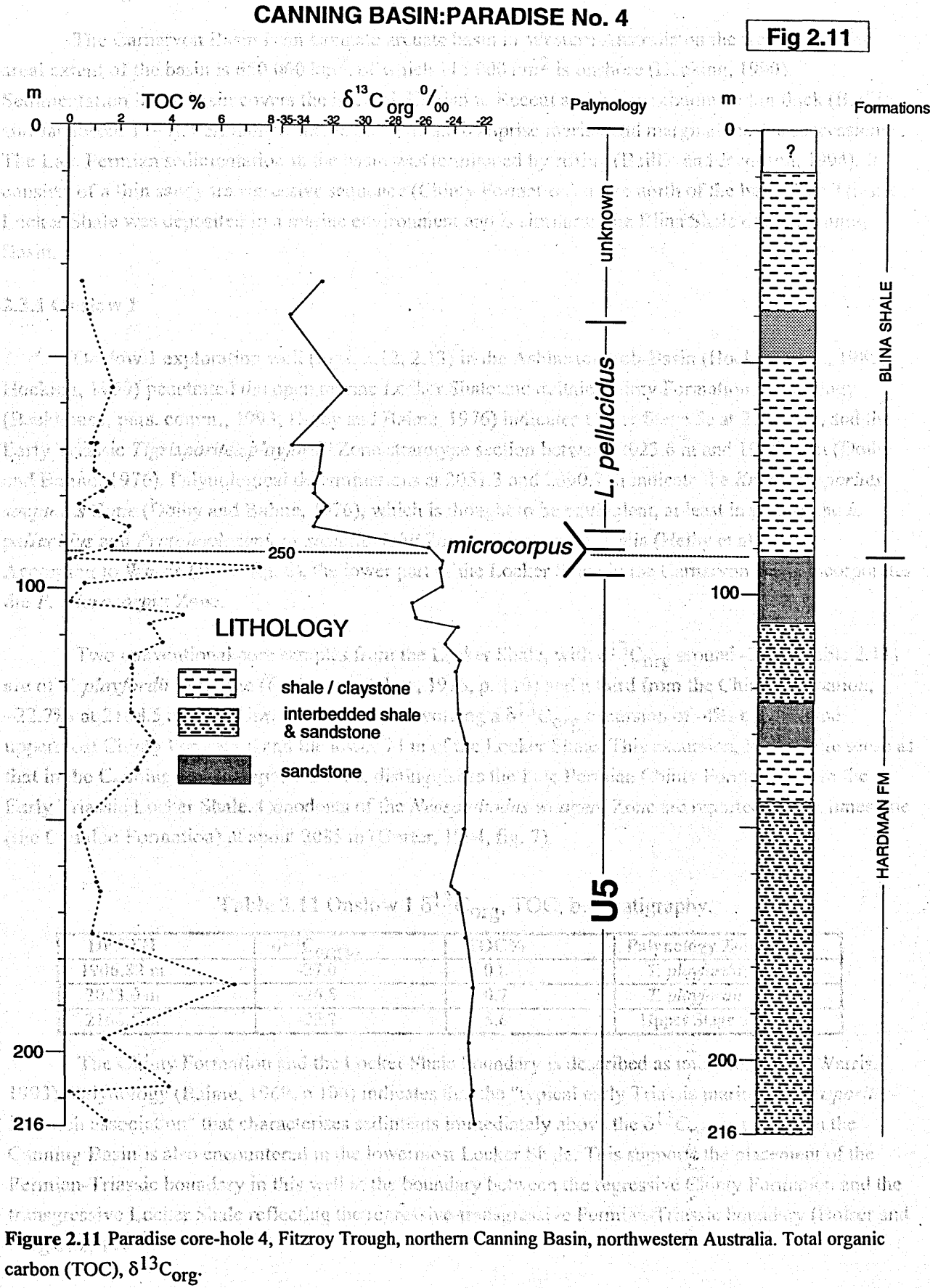


Fig. 2.11 Paradise core-hole 4



## 2.3 The Carnarvon Basin

The Carnarvon Basin is an elongate arcuate basin in Western Australia on the west coast. The areal extent of the basin is 650 000 km<sup>2</sup>, of which 115 000 km<sup>2</sup> is onshore (Hocking, 1990). Sedimentation in the basin covers the interval Silurian to Recent and is a maximum 15 km thick (Baillie and Jacobson, 1994). Permian sediments in the basin comprise marine and marginal marine successions. The Late Permian sedimentation in the basin was terminated by rifting (Baillie and Jacobson, 1994). It consists of a thin sandy transgressive sequence (Chinty Formation) in the north of the basin. The Triassic Locker Shale was deposited in a marine environment and is similar to the Blina Shale of the Canning Basin.

### 2.3.1 Onslow 1

Onslow 1 exploration well (Figs. 2.12, 2.13) in the Ashburton Sub-Basin (Hocking et al., 1985; Hocking, 1990) penetrated the open marine Locker Shale and deltaic Chinty Formation. Palynology (Backhouse, pers. comm., 1993; Dolby and Balme, 1976) indicates Upper Stage 5c at 2166.2 m, and the Early Triassic *Tigrisporites playfordii* Zone stratotype section between 2023.6 m and 1906.82 m (Dolby and Balme, 1976). Palynological determinations at 2051.3 and 2090.7 m indicate the *Kraeuselisporites saeptatus* Zone (Dolby and Balme, 1976), which is thought to be equivalent, at least in part, to the *L. pellucidus* and *Protohaploxypinus samoilovichii* Zones of eastern Australia (Helby et al., 1987). According to Warris (1993, fig. 6), the lower part of the Locker Shale in the Carnarvon Basin incorporates the *P. microcorpus* Zone.

Two conventional core samples from the Locker Shale, with  $\delta^{13}\text{C}_{\text{org}}$  around -27‰ (Table 2.11) are of *T. playfordii* Zone age (Dolby and Balme, 1976, p. 119) and a third from the Chinty Formation, -22.7‰ at 2168.5 m, is of Upper Stage 5 age, involving a  $\delta^{13}\text{C}_{\text{org}}$  excursion of -4‰ between the uppermost Chinty Formation and the lower 73 m of the Locker Shale. This excursion, in the same sense as that in the Canning and Bonaparte Basins, distinguishes the Late Permian Chinty Formation from the Early Triassic Locker Shale. Conodonts of the *Neospathodus waageni* Zone are reported from a limestone (the Cunaloo Formation) at about 2085 m (Gorter, 1994, fig. 7).

Table 2.11 Onslow 1  $\delta^{13}\text{C}_{\text{org}}$ , TOC, biostratigraphy.

DEPTH	$\delta^{13}\text{C}_{\text{org}}\text{‰}$	TOC%	Palynology Zone
1906.82 m	-27.0	0.8	<i>T. playfordii</i>
2023.6 m	-26.8	0.7	<i>T. playfordii</i>
2168.5 m	-22.7	5.6	Upper Stage 5

The Chinty Formation and the Locker Shale boundary is described as unconformable (Warris, 1993). Palynology (Balme, 1969, p.106) indicates that the "typical early Triassic marine *Taeniasporites-acritarch* association" that characterises sediments immediately above the  $\delta^{13}\text{C}_{\text{org}}$  excursion in the Canning Basin is also encountered in the lowermost Locker Shale. This supports the placement of the Permian-Triassic boundary in this well at the boundary between the regressive Chinty Formation and the transgressive Locker Shale reflecting the regressive-transgressive Permian-Triassic boundary (Holser and Magaritz, 1987).

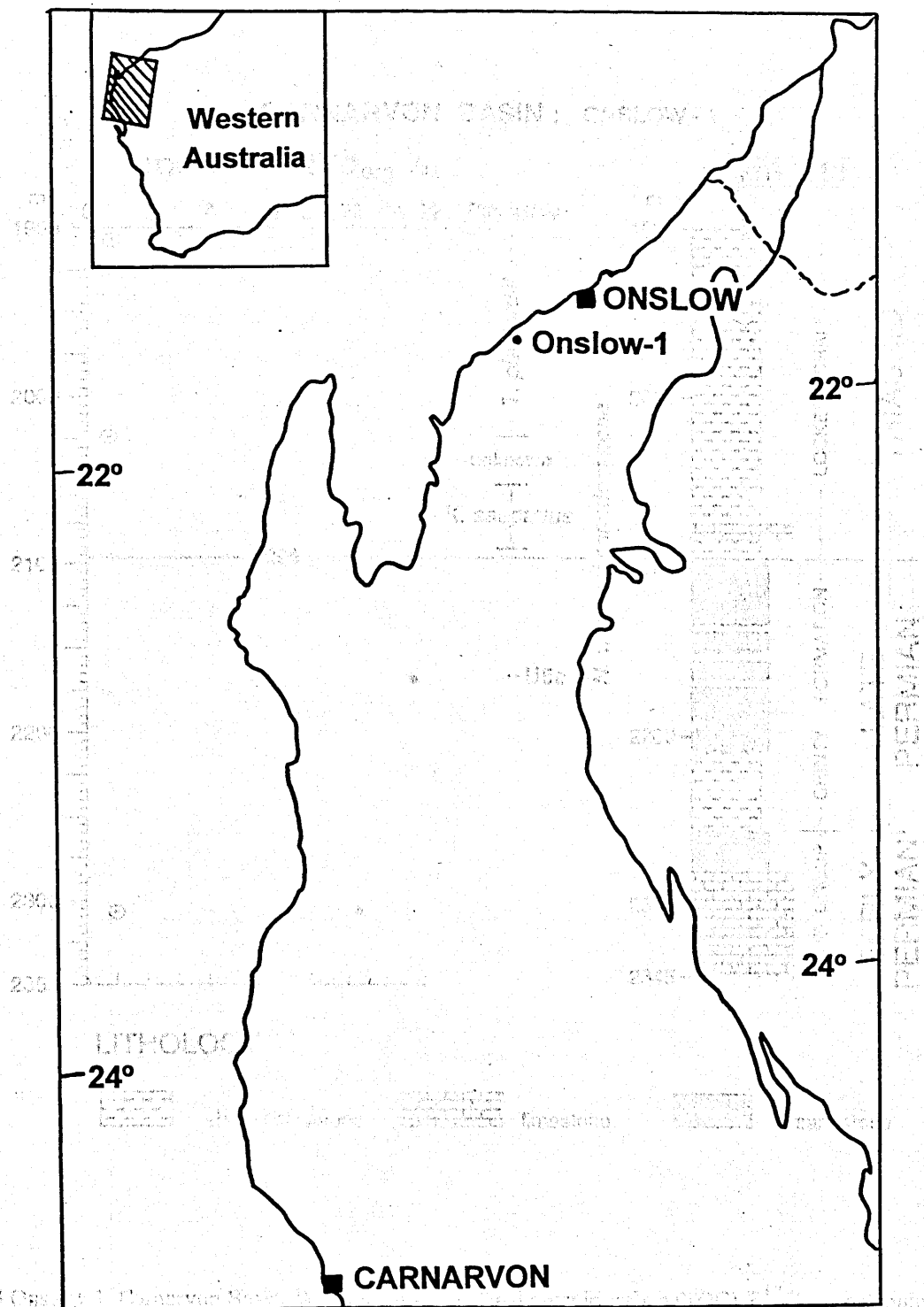


**Figure 2.12** Location of Onslow 1.

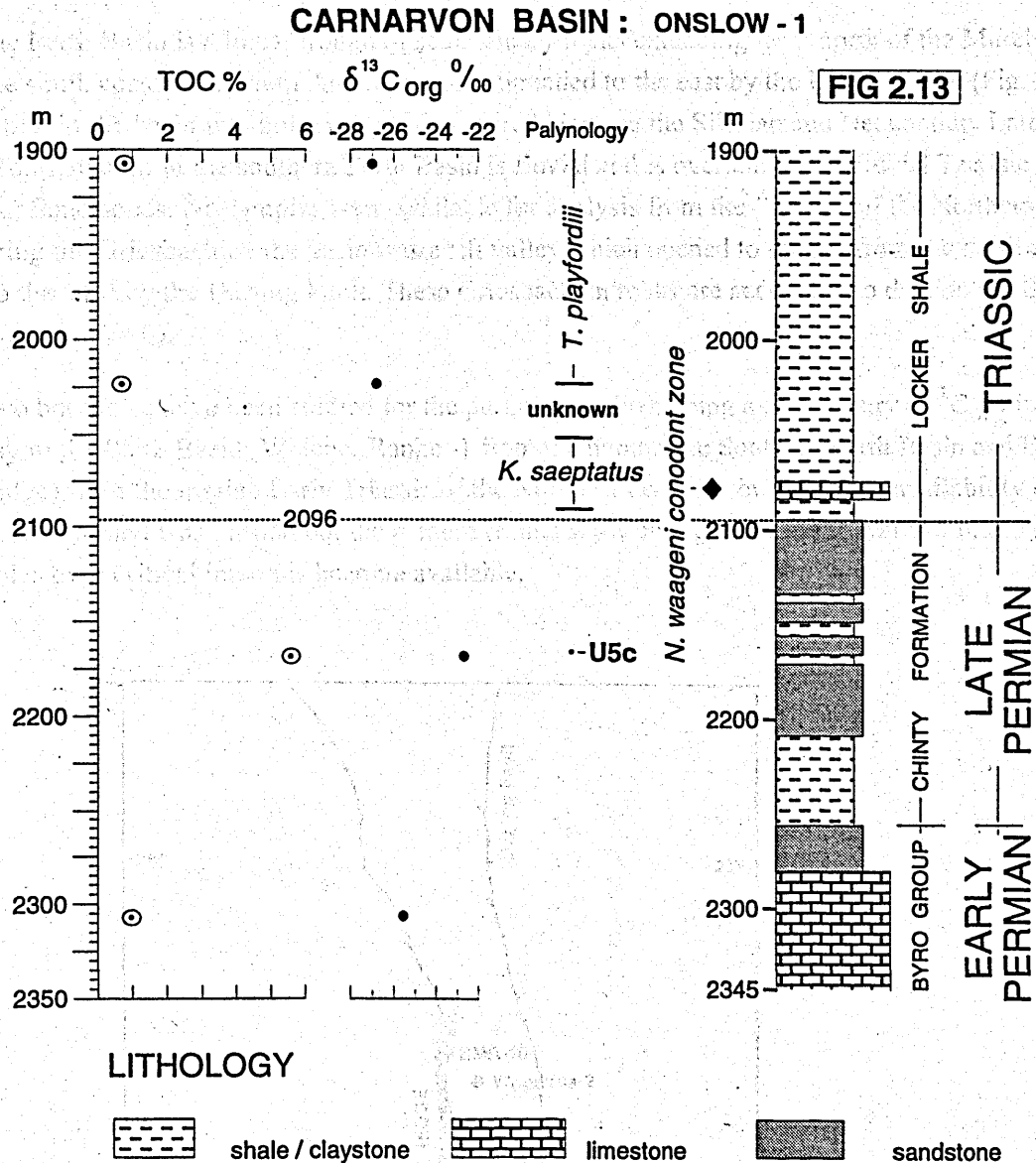


**Figure 2.13** Onslow-1, Carnarvon Basin, Western Australia. Total organic carbon (TOC),  $\delta^{13}\text{C}_{\text{org}}$ , palynological zones (J. Backhouse pers. comm., 1993a; Dolby and Balme, 1976), lithological log and formations (Warris, 1994, fig. 6; Hocking et al., 1985; Hocking, 1990).

## 2.4 Perth Basin

The Perth Basin is a linear trough of sedimentary rocks extending from north of the Murchison River to the south coast of Western Australia and is bounded to the east by the Darling Fault (Fig. 2.14). Sedimentation in the basin was polycyclic and occurred between the Silurian and Neocomian. Late Permian sedimentation in the southern Perth Basin is fluvial and is overlain by the fluvial Triassic Sabina and Lesueur Sandstones. No samples were available for analysis from the Permian of the Northern Perth Basin. During the Griesbachian the basin was a rift valley which opened to the sea from the north and was bounded to the east by the Darling Fault. These Griesbachian rocks are accessible to drill on the Beagle Ridge (Cockbain, 1990).

Two boreholes have been studied for the purposes of developing a preliminary  $\delta^{13}\text{C}_{\text{org}}$  isotope stratigraphy in the Perth Basin; Whicher Range -1 from the nonmarine Southern Perth Basin and BMR 10 (Beagle Ridge) from the marine Early Triassic of the Northern Perth Basin. Sampling availability from both boreholes studied was limited but the meagre results show enough promise to warrant future study as more samples over critical intervals become available.

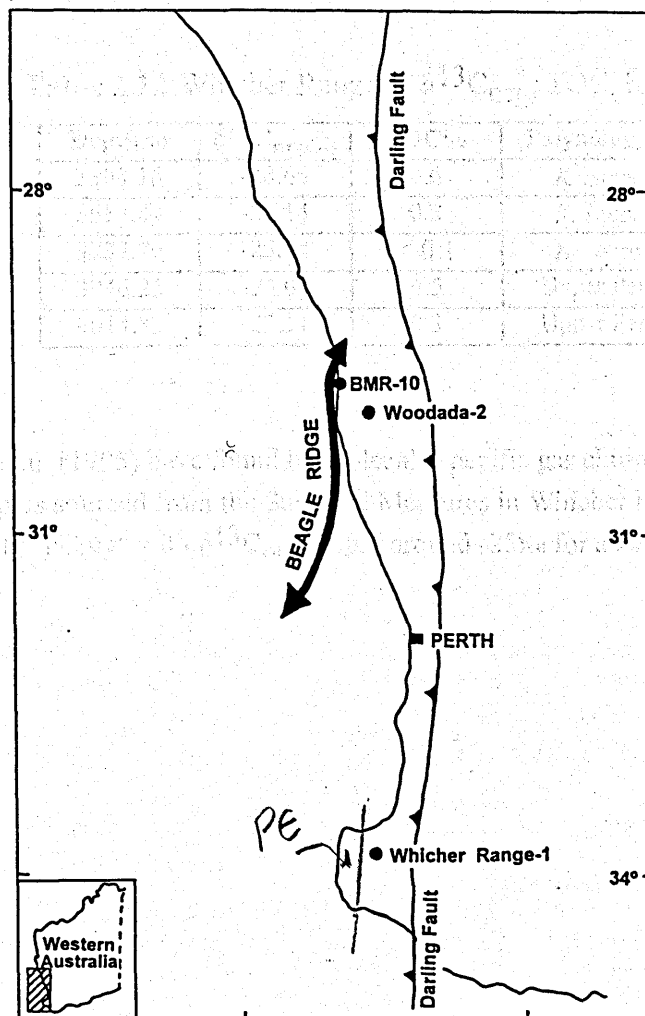


Figure 2.14 Location of BMR 10 (Beagle Ridge) and Whicher Range-1.



### 2.4.1 Whicher Range-1

Whicher Range-1 in the southern Perth Basin in the Bunbury Trough was drilled by Union Oil in 1968. A  $\delta^{13}\text{C}_{\text{org}}$  profile (Fig. 2.15, Table 2.12) has three samples in the fluvial Lesueur Sandstone and the Sabina Sandstone type section (Cockbain, 1990) and 2 samples in the uppermost Sue Coal Measures.

Samples analysed from 4014.8 m and 3946 m show  $\delta^{13}\text{C}_{\text{org}}$  typical of those in the Permian of Western Australia at around -23 to -24‰, and are tentatively assigned an Upper Permian age on the basis of palynology (Backhouse pers. comm., 1993). The vitrinite reflectance of samples around 4000 m in this well are about 0.8%  $R_{\text{Omax}}$  (Kantsler and Cook, 1979), which indicates they probably retain a primary  $\delta^{13}\text{C}_{\text{org}}$  signature. At 3737.76 m a  $\delta^{13}\text{C}_{\text{org}}$  value of -25‰ has been determined from a sample with *Aratrisporites* sp. that indicates the *K. saeptatus* Zone (Summons et al., 1995), not the *P. microcorpus* Zone as indicated in Morante et al. (1994). At 3583.84 m and 3490 m, Triassic-like  $\delta^{13}\text{C}_{\text{org}}$  values of -27.14‰ and -28.66‰ come from rocks time equivalent to the Kockatea Shale (Backhouse pers. comm., 1993). The Permian-Triassic boundary therefore lies somewhere between 3946.25m and 3737.76 m in Whicher Range-1 within the topmost Sue Coal Measures or Sabina Sandstone and is marked by an excursion in  $\delta^{13}\text{C}_{\text{org}}$  of -5.5‰. The Permian-Triassic system boundary is chosen accordingly at the boundary between these units (Fig. 2.15).

**Table 2.12** Whicher Range-1,  $\delta^{13}\text{C}_{\text{org}}$ , TOC, biostratigraphy.

Depth m	$\delta^{13}\text{C}_{\text{org}}\text{‰}$	TOC%	Palynology Zone
3493.16	-28.66	0.6	<i>K. saeptatus</i>
3583.84	-27.14	0.2	<i>K. saeptatus</i>
3737.76	-25.04	< 0.1	<i>K. saeptatus</i>
3946.25	-23.01	4.5	Upper Permian
4014.83	-23.11	0.3	Upper Permian

Summons et al. (1995) have found by molecule specific gas chromatograph-mass spectrometer analyses of oil samples sourced from the Sue Coal Measures in Whicher Range-1 that Permian organic carbon is isotopically "heavy" with  $\delta^{13}\text{C}_{\text{org}}$  values around -25‰ for alkanes in the range  $\text{C}_{17-30}$ .

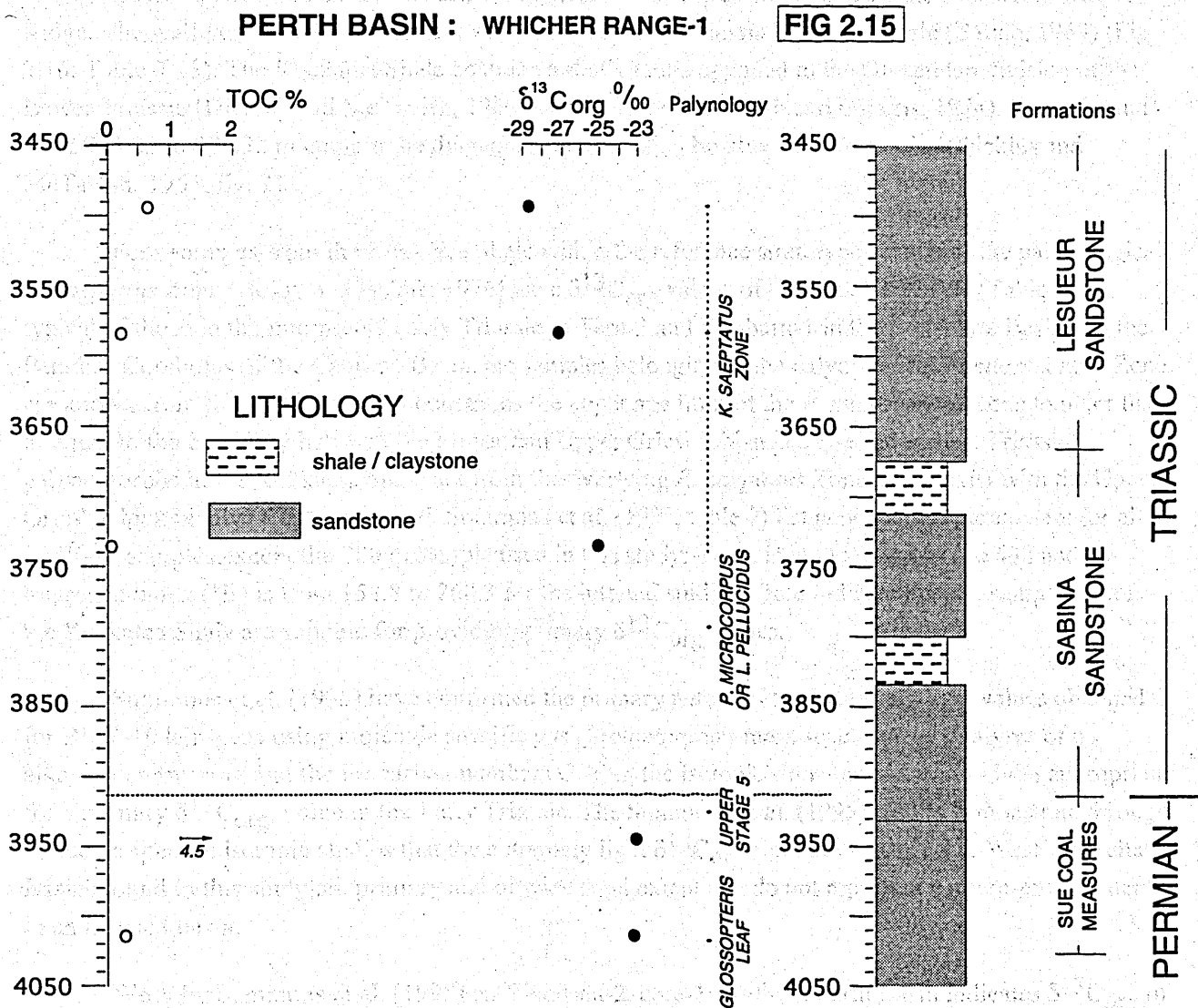


**Figure 2.15** Whicher Range-1, Perth Basin, Western Australia. Total organic carbon (TOC),  $\delta^{13}\text{C}_{\text{org}}$ , palynological zones (J. Backhouse pers. comm., 1993; Backhouse, 1993; Balme, 1968), lithological log (Veevers, 1971) and formations (Cockbain, 1990).

## 2.4.2 BMR 10 (Beagle Ridge)

BMR 10 (Beagle Ridge) was drilled by the B.M.R. in 1959 to investigate the subsurface Beagle Ridge. The well penetrated an important section of the Early Triassic Kockatea Shale (Balme, 1969) (Fig. 2.16; Table 2.13). The Kockatea Shale contains a shelly fauna assigned to the Otoceratan division of the Lower Triassic (Dickins and McTavish, 1963; Balme, 1969; McTavish and Dickins, 1974). Cores 34 and 35 at 973.22 to 979.32 m contain the diagnostic Griesbachian bivalve *Claraia stachei* (Dickins and McTavish, 1963, fig. 2).

Four samples from the Kockatea Shale within the reference stratotype section of the palynological *K. saeptatus* Zone (Dolby and Balme, 1976) have  $\delta^{13}\text{C}_{\text{Org}}$  values of -34.4‰ to -32.9‰ (Table 2.13), typical of those in the interpreted Early Triassic of Tern-3 and Fishburn-1 in the Bonaparte Basin and the Paradise Coreholes of the Canning Basin. No samples belonging to the palynological *P. microcorpus* Zone are known from this corehole. This constrains the upper age limit of the *P. microcorpus* Zone to older than or equal to the boundary between the Lower and Upper Griesbachian because the earliest Triassic palynomorphs in the Kockatea Shale are from the overlying *K. saeptatus* Zone and coexist with the Upper Griesbachian bivalve *Claraia stachei*. Summons et al. (1995, table 2) list geochemical parameters for all BMR-10 samples except the 780 m sample used in this study: Tmax is in the range 427 to 438 and the hydrogen index (HI) is from 158.8 to 268.3 for the interval studied. Both indicate that the samples from the Kockatea Shale are suitable for providing primary  $\delta^{13}\text{C}_{\text{Org}}$  values.

Summons et al. (1995) have confirmed the primary nature of the extremely light values obtained for BMR-10 kerogens using molecule specific gas chromatograph-mass spectrometer analyses of n-alkanes determining that the for carbon numbers C<sub>17-30</sub> the isotopic signature is around -34‰ appropriate for a primary  $\delta^{13}\text{C}_{\text{Org}}$  value in the Early Triassic. The Summons et al. (1995) results demonstrate through molecule specific isotopic studies that the extremely light  $\delta^{13}\text{C}_{\text{Org}}$  signatures from other West Australian Basins found in this study are primary and of wide areal extent and do not represent a micro-environment in an isolated basin.

Work by Summons et al. (1995) on Woodada-2, core-1, northern Perth Basin indicates  $\delta^{13}\text{C}_{\text{Org}}$  of -29 to -31.3‰ for kerogens in sediments with *Claraia concentrica* and *C. stachei* and for samples in sediments with ostracod *Carinaknightina discarinata* values around -29.3‰. Since *C. stachei* occurs in the Lower Chinglung Formation at Meishan in the Zhongxin Dadui Quarry (Sheng, 1984) these diagnostic Early Triassic (Upper Griesbachian) fossils (Sheng et al., 1984, table 1) indicate the age of the samples from the Kockatea Shale. This supports the interpretation by Morante et al. (1994) that  $\delta^{13}\text{C}_{\text{Org}}$  values of kerogens in sediments in the Early Triassic are very negative. This biostratigraphical correlation between the Northern Perth Basin and sections on the Paleotethyan margin and South China indicate very negative  $\delta^{13}\text{C}_{\text{Org}}$  values in the Griesbachian.

Table 2.13 BMR 10 (Beagle Ridge):  $\delta^{13}\text{C}_{\text{Org}}$ , TOC %, biostratigraphy.

DEPTH	$\delta^{13}\text{C}_{\text{Org}}\%$	TOC%	Palynology Zone
681.2 m	-34.4	0.5	<i>K. saeptatus</i>
735.9 m	-34.4	0.4	<i>K. saeptatus</i>
780 m	-32.9	0.3	<i>K. saeptatus</i>
978.3 m	-33.3	2.2	<i>K. saeptatus</i>

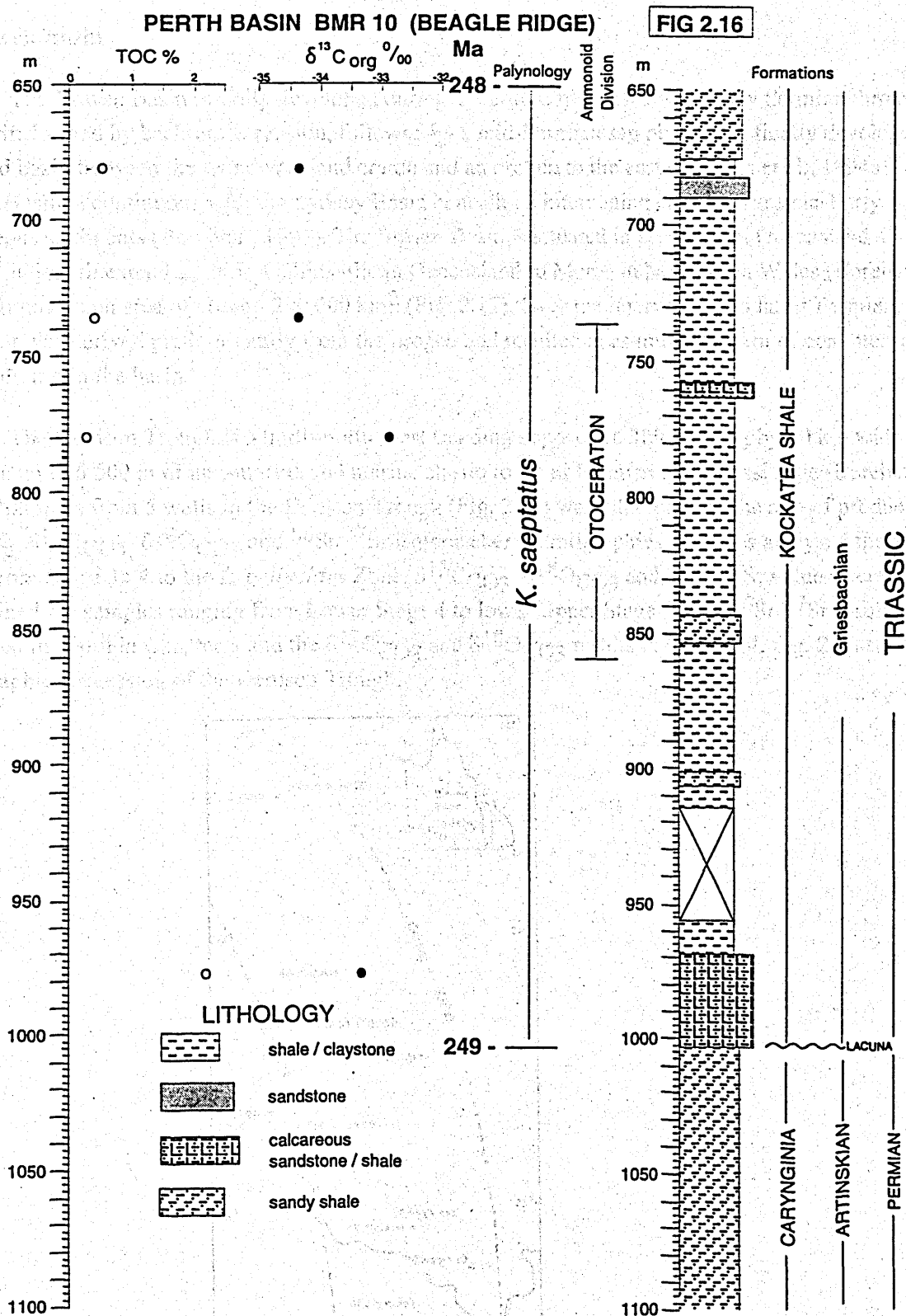


**Figure 2.16** BMR-10 (Beagle Ridge), Perth Basin, Western Australia. Total organic carbon (TOC),  $\delta^{13}\text{C}_{\text{org}}$  (relative to PDB), palynological zones (Dolby and Balme, 1976), lithological log, and formations (McTavish, 1965).  $\delta^{13}\text{C}_{\text{org}}$  has a mean value of -33.75‰ for the Early Triassic. The Kockatea Shale is Griesbachian in the Otoceratan division of Spath (Balme, 1969), and the Carynginia Formation is Artinskian (Cockbain, 1990) or Artinskian/Kungurian (Summons et al., 1995, fig. 2).

## 2.5 Bowen Basin

The Bowen Basin initially developed during the Late Carboniferous or Early Permian through an initial rift formed by back-arc extension, followed by a mid-Permian sag phase, and finally developed as a foreland basin between the Gondwanaland craton and an orogen to the east (Veevers et al., 1994a). The Bowen Basin is continuous with the Sydney Basin beneath an intervening cover of Jurassic-Early Cretaceous sediments (Boreham, 1995). The Bowen Basin is situated in east-central Queensland and is 900 km in length extending from Collinsville in Queensland to Moree in New South Wales (Boreham, 1995). It covers an area of around 200 000 km<sup>2</sup> (Fig. 2.17). Over the interval mid to latest Permian, sediment was derived predominantly from the orogen and resulted in as much as 5 km of coal measures accumulating in the basin.

The Denison Trough is a north-north-west trending depocentre 320 km long by 60 km wide that contains up to 6 500 m of non-marine and marine clastic rocks of Permian and Triassic age (Boreham, 1995). Samples from 5 wells in the Denison Trough (Fig. 2.17) were studied with the aim of producing  $\delta^{13}\text{C}_{\text{org}}$ ,  $\delta^{13}\text{C}_{\text{CO}_3}$ ,  $\delta^{18}\text{O}_{\text{CO}_3}$  and  $^{86}\text{Sr}/^{87}\text{Sr}$  isotope chemostratigraphies. Samples analysed for  $\delta^{13}\text{C}_{\text{org}}$  range from Stage 3b/4 to the *L. pellucidus* Zone.  $\delta^{13}\text{C}_{\text{CO}_3}$ ,  $\delta^{18}\text{O}_{\text{CO}_3}$  and  $^{86}\text{Sr}/^{87}\text{Sr}$  values were determined for samples ranging from Lower Stage 4 to lower Upper Stage 5. The  $^{86}\text{Sr}/^{87}\text{Sr}$  results are discussed in detail in Chapter 3 and the  $\delta^{13}\text{C}_{\text{CO}_3}$  and  $\delta^{18}\text{O}_{\text{CO}_3}$  results in Chapter 4. Fig. 2.18 shows the stratigraphic succession of the Denison Trough.

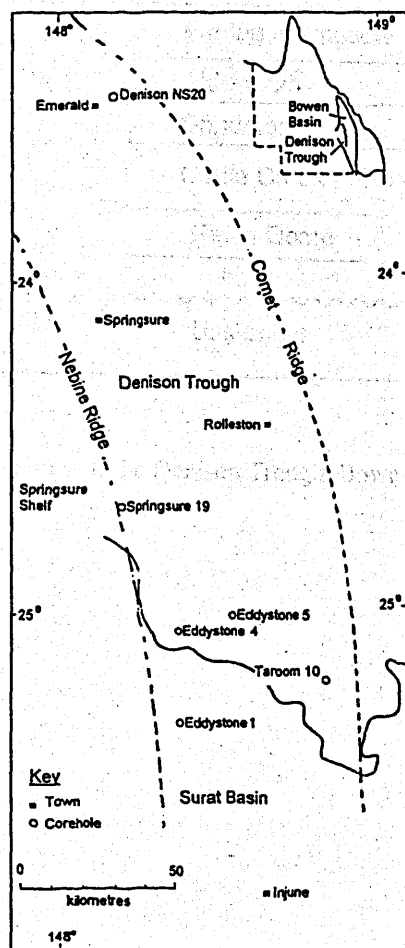
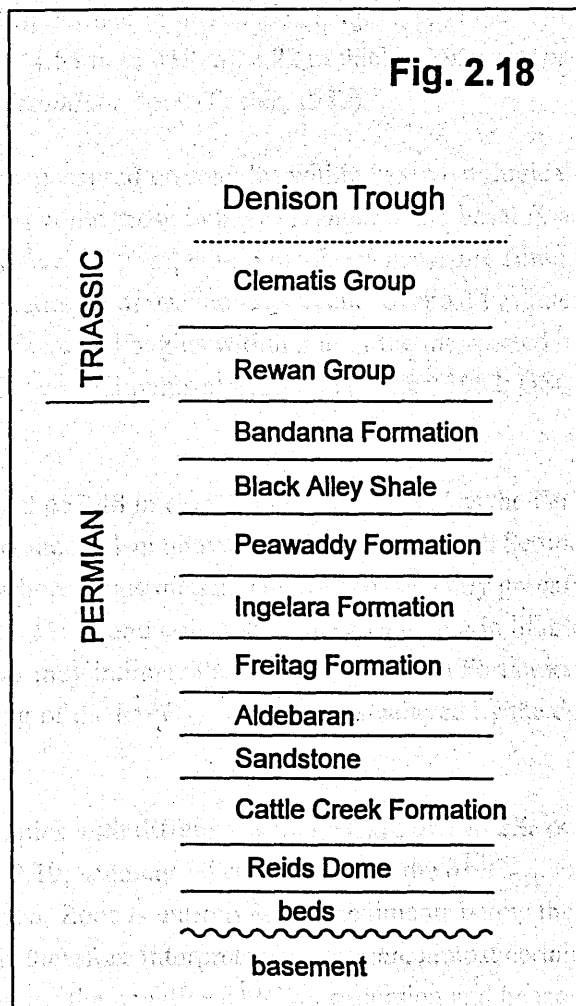


Figure 2.17 Location of Denison NS 20, Eddystone 1, Eddystone 5, Taroom 10 and Springsure 19.

Year	Percentage
1900	4
1920	6
1940	8
1960	10
2000	14

**Fig. 2.18**



**Figure 2.18 Generalised stratigraphy of the Denison Trough, Bowen Basin after Boreham (1995).**

### 2.5.1 Denison NS20

Denison NS20 corehole in the Denison Trough, drilled in 1978 by the Queensland Geological Survey, penetrated the nonmarine Early Triassic Rewan Group and the underlying Permian Rangal Coal Measures (Foster, 1982; GSQ Denison NS20 coal section geological log, 1978, unpublished). The palynology zones are well defined in this section (Fig. 2.19, Table 2.14) and include a 264.5 m thick *L. pellucidus* Zone (from 174.55 m to 439 m), a 22 m thick *P. microcorpus* Zone, and the stratotype section of the *Playfordiaspora crenulata* Zone (Foster, 1982).

$\delta^{13}\text{C}_{\text{org}}$  values measured on samples within the palynological zone Upper Stage 5 are generally more positive than  $-24\text{‰}$  while those in the *P. crenulata* and basal *P. microcorpus* Zone lie between  $-24\text{‰}$  and  $-25.16\text{‰}$ . Above 448.9 m, within the *P. microcorpus* Zone, a change to more negative values occurs. This  $\delta^{13}\text{C}_{\text{org}}$  excursion of around  $-5\text{‰}$  occurs over a 14 m interval within the *P. microcorpus* Zone and *L. pellucidus* Zone and begins within 5 m of the interpreted boundary between coal measures and overlying Rewan Group sediments at 453.48 m (Foster, 1982; GSQ Denison NS20 coal section geological log, 1978).

The dotted line at 453.48 m (Fig. 2.19) is interpreted as the Permian-Triassic boundary at the base of the Rewan Formation, about 1 m above the highest coal band. Sediments between 453.5 m and 447.8 m are still greyish with carbonaceous matter. The first consistently green/grey sediments begin after 447.8 m (core store observations, 1992) and coincide with a coarsening in lithology and the beginning of the  $\delta^{13}\text{C}_{\text{org}}$  excursion. This may indicate the base of the Rewan Formation may be misplaced in this core-hole or that the incoming of the  $\delta^{13}\text{C}_{\text{org}}$  excursion is delayed by the dominance of reworked "Permian", organic matter.

Juxtaposed samples with differences in  $\delta^{13}\text{C}_{\text{org}}$  of 1 to 2‰ occur in the coal measures but the  $-5.5\text{‰}$  excursion (Fig. 2.19, segment B) correlates with the  $\delta^{13}\text{C}_{\text{org}}$  excursions in sections elsewhere in Australia. The *P. crenulata* Zone is entirely within sediments below the negative  $\delta^{13}\text{C}_{\text{org}}$  excursion (Fig. 2.19, segment A) and is therefore interpreted as Permian, almost certainly latest Permian. The *P. microcorpus* Zone contains the negative  $\delta^{13}\text{C}_{\text{org}}$  excursion and hence straddles the Permian-Triassic boundary. This differs from the interpretation of Foster (1982) that the *P. crenulata* Zone is "Middle Permian" = to Early Djulfian in age and that the *P. microcorpus* Zone is entirely Permian. According to Foster (1982, p. 176) the *P. crenulata* Zone "seems to represent the ultimate expression of the *Glossopteris* megafloral remains in the succession" and (Foster, 1982, p.182) "its presence emphasises the continuity of microfloral/floral succession" between the Upper Stage 5 and *P. microcorpus* zones. Because the negative  $\delta^{13}\text{C}_{\text{org}}$  excursion indicates the Permian-Triassic boundary the *P. crenulata* Zone indicates a significant environmental change approaching the Permian-Triassic boundary. The *P. crenulata* Zone is succeeded by the *P. microcorpus* Zone which is at the base of the *Falcisporites* Superzone which represents a major floral turnover (Retallack et al., in press) indicating the effect of the Permian-Triassic extinction on land. *P. crenulata* Zone is below the  $\delta^{13}\text{C}_{\text{org}}$  excursion in Denison NS20 and is therefore concluded to be Permian. Unit 4 of the Chhidru formation, Salt Range (Fig. 1.1) is accordingly also Permian. If Dolby and Balme (1976) are correct in assigning the Kathwai Member to the *K. saeptatus* Zone (Griesbachian in the Perth Basin) this implies the hiatus between Unit 4 and the Kathwai Member may be  $\geq$  the *P. microcorpus* Zone.

Table 2.14 Denison NS 20.  $\delta^{13}\text{C}_{\text{org}}$ , TOC, biostratigraphy.

Corehole	Depth (m)	$\delta^{13}\text{C}_{\text{org}}\text{‰}$	TOC%	Sample type	Palynological Zone
DNS20	360	-29.64	0.7	cc	<i>L. pellucidus</i>
DNS20	362	-27.48	0.5	cc	<i>L. pellucidus</i>
DNS20	362	-27.66	0.5	cc	<i>L. pellucidus</i>
DNS20	372.6	-30.12	4.1	cc	<i>L. pellucidus</i>
DNS20	383.3	-27.93	10	cc	<i>L. pellucidus</i>
DNS20	383.3	-28.14	1.2	cc	<i>L. pellucidus</i>
DNS20	383.3	-28.14	1.2	cc	<i>L. pellucidus</i>
DNS20	389.5	-28.74	1.2	cc	<i>L. pellucidus</i>
DNS20	391.4	-28.62	1.1	cc	<i>L. pellucidus</i>
DNS20	395.6	-29.66	1.5	cc	<i>L. pellucidus</i>
DNS20	397.5	-29.63	0.8	cc	<i>L. pellucidus</i>
DNS20	397.5	-28.54	0.8	cc	<i>L. pellucidus</i>
DNS20	397.5	-28.76	1.0	cc	<i>L. pellucidus</i>
DNS20	407.7	-28.75	2.1	cc	<i>L. pellucidus</i>
DNS20	407.7	-29.22	1.6	cc	<i>L. pellucidus</i>
DNS20	414	-28.91	1.5	cc	<i>L. pellucidus</i>
DNS20	414	-28.77	1.1	cc	<i>L. pellucidus</i>
DNS20	414.4	-29.33	1.1	cc	<i>L. pellucidus</i>
DNS20	418.3	-28.38	1.0	cc	<i>L. pellucidus</i>
DNS20	427	-31.13	< 0.1	cc	<i>L. pellucidus</i>
DNS20	434.3	-30.12	0.5	cc	<i>L. pellucidus</i>
DNS20	435.5	-30.18	1.1	cc	<i>L. pellucidus</i>
DNS20	435.5	-30.34	1.1	cc	<i>L. pellucidus</i>
DNS20	438.9	-30.17	0.8	cc	<i>P. microcorpus</i>
DNS20	439.88	-27.90	0.5	cc	<i>P. microcorpus</i>
DNS20	442	-26.41	0.7	cc	<i>P. microcorpus</i>
DNS20	442.18	-26.15	0.5	cc	<i>P. microcorpus</i>
DNS20	443.6	-26.73	0.1	cc	<i>P. microcorpus</i>
DNS20	444.3	-26.61	0.2	cc	<i>P. microcorpus</i>
DNS20	445.6	-26.32	0.3	cc	<i>P. microcorpus</i>
DNS20	446.4	-25.01	0.4	cc	<i>P. microcorpus</i>
DNS20	447.9	-24.63	0.7	cc	<i>P. microcorpus</i>
DNS20	448.9	-23.75	0.2	cc	<i>P. microcorpus</i>
DNS20	451	-25.53	0.4	cc	<i>P. microcorpus</i>
DNS20	451	-25.58	0.4	cc	<i>P. microcorpus</i>
DNS20	452	-24.75	1.4	cc	<i>P. microcorpus</i>
DNS20	453	-24.82	1.4	cc	<i>P. microcorpus</i>
DNS20	453	-24.71	1.4	cc	<i>P. microcorpus</i>
DNS20	453.9	-24.71	7.5	cc	<i>P. crenulata</i>
DNS20	454.77	-25.16	9.8	cc	<i>P. crenulata</i>
DNS20	455.79	-24.82	2.2	cc	<i>P. crenulata</i>
DNS20	457.55	-24.96	2.3	cc	<i>P. crenulata</i>
DNS20	460.57	-25.16	5.0	cc	<i>P. crenulata</i>
DNS20	461.5	-23.44	0.8	cc	<i>P. crenulata</i>
DNS20	465.12	-26.05	3.5	cc	Upper Stage 5
DNS20	465.85	-23.88	2.0	cc	Upper Stage 5
DNS20	467.65	-23.93	1.6	cc	Upper Stage 5
DNS20	468.37	-23.80	2.1	cc	Upper Stage 5
DNS20	469.33	-24.38	4.3	cc	Upper Stage 5
DNS20	475.59	-22.67	1.1	cc	Upper Stage 5
DNS20	483.2	-22.97	1.8	cc	Upper Stage 5



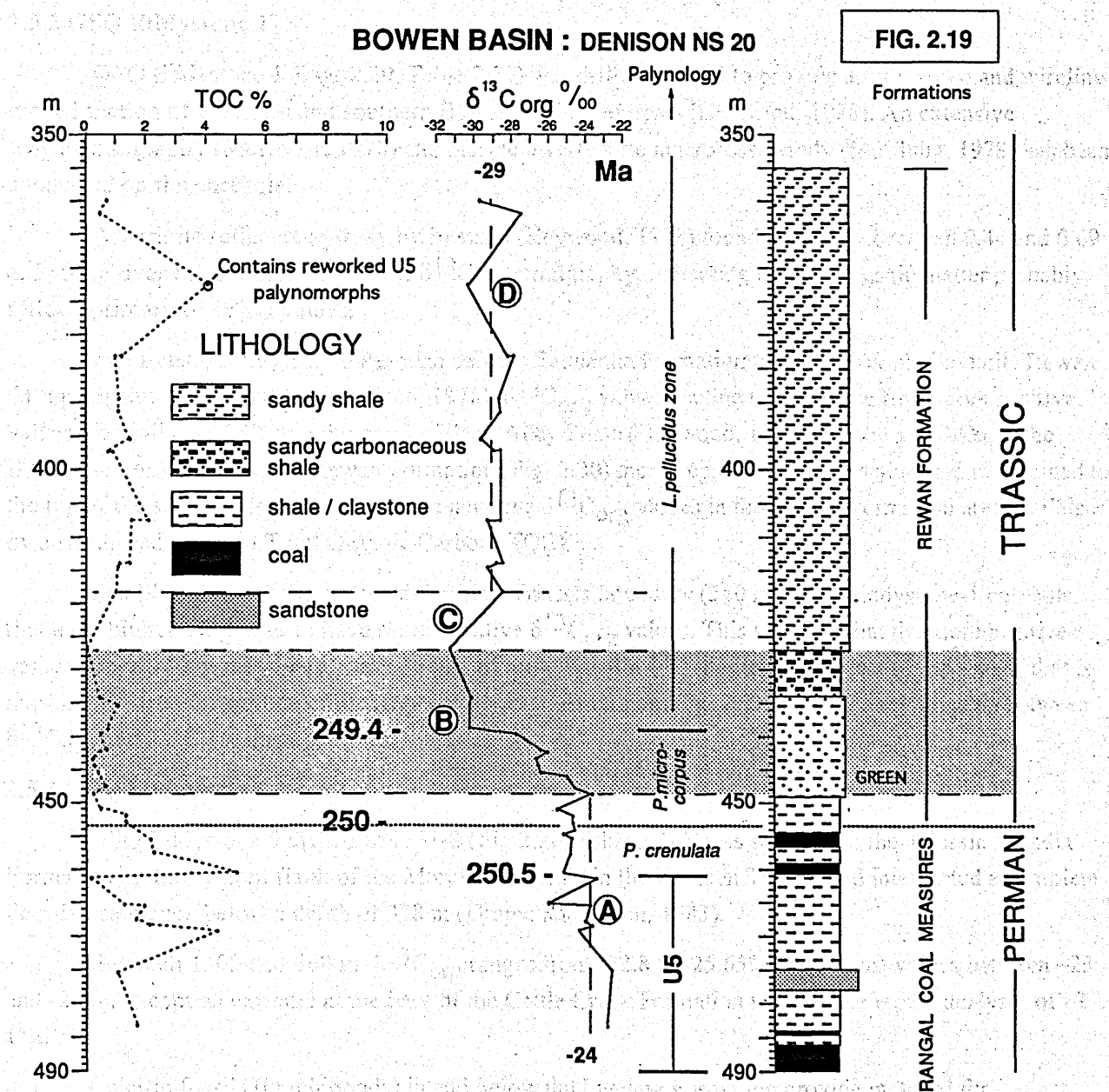


**Figure 2.19** Denison NS 20, Bowen Basin, eastern Australia. Total organic carbon (TOC),  $\delta^{13}\text{C}_{\text{org}}$ , palynological zones (Foster, 1982), lithological log, and formations (GSQ Denison NS20 coal section geological log, 1978). The negative excursion in  $\delta^{13}\text{C}_{\text{org}}$  is between mean values of -24 ‰ for the Permian and -30 ‰ for the Triassic and is within the *P. microcorpus* Zone that extends from 461.75 m to 439 m (Foster, 1982, fig. 5). The interval of the  $\delta^{13}\text{C}_{\text{org}}$  excursion (B) is shaded. The *Playfordiaspora crenulata* Zone extends from 461.75 m to 453.48 m (Foster, 1982, p.173, not as in fig. 5, p. 175). The dotted line at 453.48 m is my pick of the Permian-Triassic boundary.